tissues have shown that odontoblast differentiation is controlled by the inner dental epithelium (Ruch et al., 1982; Kollar, 1985; Thesleff et al., 1989). Odontoblasts are columnar polarized cells with eccentric nuclei and long cellular processes, and this cytological polarization specifically occurs in a single cell layer adjacent to the basement membrane of the inner dental epithelium (Linde and Goldberg, 1993). The terminal differentiation of odontoblasts is initiated during the bell stage of tooth morphogenesis at the sites of the future cusps (Lesot et al., 2001; Thesleff et al., 2001). The patterning of the cusps, on the other hand, is determined by the positions of the secondary enamel knots, epithelial signaling centers resembling other embryonic signaling centers, such as the notochord and the apical ectodermal ridge in limbs (Jernvall et al., 1994; Jernvall and Thesleff, 2000). The cells of the enamel knots are non-proliferative, and they express several signaling molecules. These signals may control the folding of the inner enamel epithelium and as odontoblast differentiation starts from the mesenchymal cells underlying enamel knots it has been suggested that signals from the secondary enamel knots may also determine the location and time of the onset of odontoblast terminal differentiation (Thesleff et al., 2001). However the molecular mechanisms of the induction of odontoblast differentiation have remained unknown.

Dentin and bone share many extracellular matrix proteins associated with mineralization such as dentin matrix protein 1, fibronectin, collagen type I, alkaline phosphatase, osteonectin, osteopontin, bone sialoprotein, bono-1, and osteocalcin (Tsukamoto et al., 1992; Nakashima et al., 1994; Shiba et al., 1998; James et al., 2004). Dentin sialophosphoprotein (Dspp) is a non-collagenous extracellular matrix protein that is specifically expressed by odontoblasts (D'Souza et al., 1997). Dspp is a phosphorylated parent protein that is cleaved post-translationally into two proteins: dentin sialoprotein (Dsp) and dentin phosphoprotein (Dpp) (Feng et al., 1998). *In situ* hybridization and other experimental analyses have shown that *Dspp* is expressed predominantly in odontoblasts, transiently in preameloblasts, and at low levels in osteoblasts (D'Souza et al., 1997; Qin et al., 2002). In humans, several mutations have been identified in patients with dentinogenesis imperfecta, which is an autosomal dominant disorder of the tooth that specifically affects dentin biomineralization (Shields et al., 1973; Xiao et al., 2001; Zhang et al., 2001; Rajpar et al., 2002). A similar phenotype is found in *Dspp* null mutant mice, which feature a disturbance of dentin mineralization without any influences on bone (Sreenath et al., 2003). Hence, it is established that Dspp has a crucial role in the formation of mineralized dentin. Although the importance of epithelial–mesenchymal interactions and extracellular matrix for odontoblast differentiation is established, the molecular mechanisms of the interactions mediating odontoblast differentiation and inducing *Dspp* expression are not known.

Wnt genes encode a large family of secreted signaling proteins that specify various cell lineage pathways in development. Wnt proteins are now recognized as one of the major families of developmentally important signaling molecules and they regulate such intriguing processes as embryonic induction, the generation of cell polarity, and the specification of cell fate (Cadigan and Nusse, 1997; Nusse, 2003). In early tooth development, several Wnt genes are expressed from the initiation stage to the early bell stage (Sarkar and Sharpe, 1999). Targeted inactivation of lymphoid enhancer factor-1 (LEF1), a nuclear mediator of Wnt signaling, results in an arrest of tooth development at the bud stage (van Genderen et al., 1994). LEF1 serves as a relay of a Wnt signal to a fibroblast growth factor signal in the enamel knot in the dental epithelium, which establishes a network of reciprocal and sequential signaling between epithelium and mesenchyme (Kratochwil et al., 2002).

Here we provide evidence that Wnt10a signaling may be involved in odontoblast terminal differentiation, and based on the expression pattern of *Wnt10a*, we suggest that it has a role in linking tooth morphogenesis and odontoblast differentiation.

Materials and methods

Materials

Lipofectamine Plus was obtained from Gibco BRL (Gaithersburg, MD). Biocoat Matrigel-coated dishes were from Becton Dickinson (Labware, MA). The rabbit polyclonal anti-Wnt10a antibody was produced by Sigma Genosys Co. (Hokkaido, Japan) using a synthetic peptide as antigen, which was established by the Wnt10a protein sequence analysis (U61969). The amino acid sequence of the antigen peptide is RRGDEEAFRRKLHR and corresponds to amino acids 163–176 of the Wnt10a protein. All other chemicals were analytical grade.

Processing of tissues

Wild-type mouse embryos were obtained from the NMRI strain. Heads of embryonic E12, E13, E14, and E16 mice and postnatal 14 day old mice were dissected in Dulbecco's phosphate-buffered saline. The tissues were fixed in 4% paraformaldehyde at 4°C overnight. P14 heads were decalcified in 12.5% ethylene-diamine-tetra-acetic acid (EDTA) for 3 weeks. They were dehydrated, embedded in paraffin and serially sectioned at 7 μm.

Probes and *in situ* hybridization

The mouse *Wnt10a* cDNA was kindly provided by Dr Andrew P. McMahon, Harvard University, Boston, MA. Mouse *Dspp* probes were generated from A 550 bp *Dspp* fragment spanning the region between 656 and 1205 in accession # NM010080. The preparation of Bmp3 RNA probes has previously been described (Aberg et al., 1997). *In situ* hybridization of paraffin sections using 35S-UTP-labeled riboprobe was performed as described previously (Vainio

et al., 1993). The bright field and dark field images of each section were digitized, and the grains from dark fields were selected, colored red, and added to the bright field pictures in PhotoShop 6 (Åberg et al., 1997). Keratin was used as a marker for epithelial cells and it was detected by immunohistochemistry using polyclonal pan-keratin antibodies (DAKO, A575, Glostrup, Denmark) (Yamashiro et al., 2003).

Cell cultures

C3T10T1/2 cell lines, derived from embryonic mouse mesenchyme, were obtained from Riken cell bank (Tsukuba, Japan). These cells were cultured in Dulbecco's modified Eagle's medium (D-MEM, high glucose (4,500 mg/l D-glucose), with L-glutamine, and phenol red) supplemented with 0.1 mM non-essential amino acids (NEAA), 10% fetal bovine serum (FBS), 100 units U/ml penicillin, 100 µg/ml streptomycin, and incubated at 37°C in a 5% carbon dioxide, 95% air, humidified atmosphere. The cells were subcultured every 3–4 days, using 0.05% (w/v) EDTA to detach cells from the culture dish.

Wnt10a transfection in C3T10T1/2 cells

Mammalian expression vectors encoding mouse Wnt10 were constructed for transient transfections. Full-length mouse *Wnt10a* cDNA (Wang and Shackleford, 1996), pj32 was kindly provided by Dr. Gregory M. Shackleford, University of Southern California, Los Angeles, CA. *Wnt10a* was transferred from pj32 to the multiple cloning site of pCMV-Script (Stratagene, La Jolla, CA) with the restriction sites *Eco*RI and *Xho*I to generate pCMV-Wnt10a. Cells (60%–80% confluence) were transiently transfected with Lipofectamine Plus reagent (Gibco BRL, Gaithersburg, MD) according to the manufacturer's instructions. Briefly, pCMV-Wnt10a was mixed with Plus reagent in Opti-MEM I and incubated at room temperature for 15 min. Lipofectamine was mixed with DNA plus reagent and incubated further at room temperature for 15 min. Then the Lipofectamine Plus cDNA complex was added to the cells and incubated at 37°C. The control cells received Lipofectamine Plus alone. After 5 hr of incubation, growth medium containing 20% FBS was added for a final concentration of 10% FBS. The cells were maintained for an additional 12 hr. One day after transfection, cells were plated on Matrigel-coated dishes (Biocoat, Becton Dickinson Labware, Bedford, MA) or conventional culture dishes (Falcon, Becton Dickinson Labware).

Western blot analysis of Wnt10a

Cell lysate proteins (10 µg) from transfected cells were separated using 7.5% sodium dodecyl sulfate-polyacrylamide gel electrophoresis (SDS-PAGE) and were electrophoretically transferred from gel to polyvinylidene difluoride membranes. To separate non-specific protein binding, the membranes were incubated in 10 mM Tris HCl, pH 7.5, 100 mM NaCl, and 0.1% Tween 20 (TBST) containing 3% blot-qualified bovine serum albumin for 1 hr. The membranes were incubated in TBST containing a 1:1,000 diluted anti-Wnt10a antibody (Sigma Genosys Co, Hokkaido, Japan). Wnt10a polyclonal rabbit antibody was produced by Sigma Genosys Co based on the Wnt10a sequence CRRGDEEAFRR KLHR. Wnt10a antibody recognizes a band of approximately 48 kDa that corresponds to the size of Wnt10a in Wnt10a-transfected cells, while mock-transfected cells gave no signal (Fig. 2B). This signal disappeared after preincubation of the antibody with excess antigenic peptide CRRGDEEAFRRKLHR indicating that the band is specific.

The membrane was washed twice for 15 min each with 0.1% TBST, and incubated for 45 min with the secondary antibody, horseradish peroxidase (HRP)Rabbit-conjugated goat anti-rabbit (Amersham, Amersham, UK). Bound antibodies were visualized by chemiluminescence using an ECL Western Immunoblotting Kit (Amersham).

Reverse-transcriptase polymerase chain reaction (RT-PCR) of *Dspp* and *Wnt10a*

To determine whether *Wnt10a* overexpression in C3H10T1/2 cells induces *Dspp* expression, real-time PCR amplification of *Dspp* was performed. Five, ten and fifteen days after transfection, total RNA was isolated using the RNeasy-kit (Qiagen, Valencia, CA) according to the manufacturer's instructions. First molar tooth germs of the mandible from day 1 postnatal mouse pups were dissected in Dulbecco's PBS under a stereomicroscope. Total RNA was also isolated from tooth germs using the RNeasy-kit (Qiagen). Total RNA (1 µg) was reverse transcribed in 20 µl of transcription buffer [75 mM KCl, 50 mM Tris/HCl pH 8.3, 10 mM dithiothreitol, 3 mM $MgCl_2$, 0.5 mM deoxyribonucleotide trisphosphate, 1 µg oligo(dT)18-adapter primer] with Superscript II reverse transcriptase (200 U) for 1 hr at 42°C. Presence of *Dspp* and *Wnt10a* mRNA was determined using the LightCycler System and the Faststart DNA Master SYBR Green I kit (both from Roche Diagnostics, Mannheim, Germany). PCRs were performed according to the manufacturer's instructions with 0.5 µm each of the respective forward and reverse primers, 4 mM $MgCl_2$, and 1 × Faststart DNA Master SYBR Green I mix in a total volume of 20 µl. Cycling conditions were as follows: 10 min at 94°C, followed by 40 cycles with 15 sec C at 94°C, 10 sec at 64°C and 45 sec at 72°C. Standard GAPDH RT-PCR was used as an internal control for an adequate PCR reaction (472 bp). The following primers were used: 5′-atagcaccaaccatgag gct-3′ and 5′-cttttgttgcctttgttggg-3′ for *Dspp* gene, 5′-aactttggcattgt ggaagg-3′ and 5′-ggtcctcagtgtagcccaag-3′ for *Wnt10a*, 5′-aactttggc attgtggaagg -3′ and 5′-ccctgttgctgtagccgtat-3′ for GAPDH gene. PCR primer set for Dspp was designed for controlling the genomic DNA contamination. Primers that span intron–exon boundaries amplify a product from contaminating DNA that includes the intron, making it larger than the expected cDNA product. The products from the reactions described above were also run on a 1% (w/v) agarose gel, to confirm that all products were of the correct length for the primers used. After amplification, melting curve analysis of the PCR product was used to differentiate between specific and non-specific amplification products. Melting curve was acquired by heating the product at 20°C/sec to 95°C, cooling it at 20°C/sec to 55°C for 30 sec, and slowly heating it at 0.1 µC/sec to 94°C under continuous fluorescence monitoring. Melting curve analysis was accomplished with LightCycler software.

Results

Expression of *Wnt10a* and *Dspp* in the developing root

We evaluated the mRNA expression of several Wnt genes during root development at postnatal day 14, and found that *Wnt10a* transcripts were specifically present in the dental mesenchymal cells lining the inner dentin surface (Fig. 1A). *Dspp* mRNA was specifically expressed in odontoblasts (Fig. 1B), as shown previously (D'Souza et al., 1997; Bleicher et al., 1999), and both *Wnt10a* and *Dspp* were absent in the dental papilla cells, osteoblasts and cementoblasts.

The epithelial root sheath is a two-cell layer sheet at the apical end of the growing root and it regulates root growth as well as odontoblast differentiation. The root sheath can be visualized by immunohistochemistry

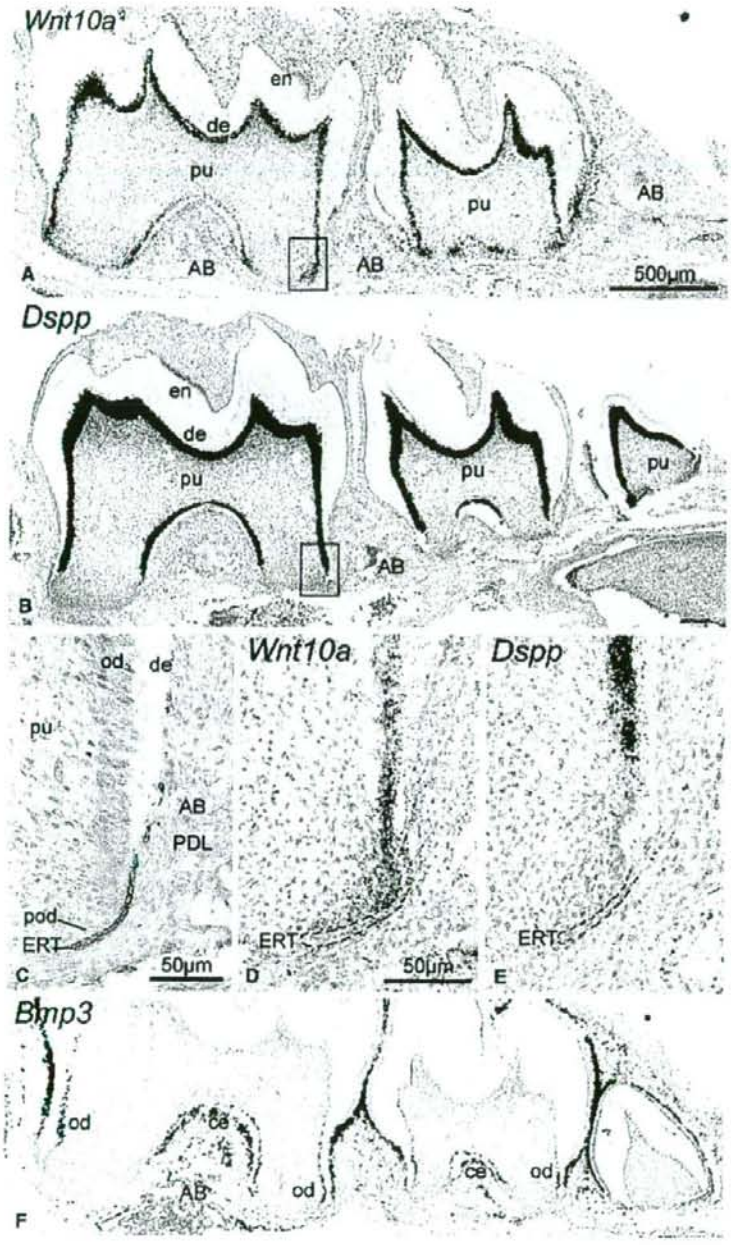

Fig. 1 Wnt10a and Dspp mRNA expression in lower jaw sections of a 14-days-old mouse (**A**, **B**) *Wnt10a* transcripts were specifically present in the odontoblasts lining the dentin (de) surface but not in the dental papilla cells (pu), or osteoblasts in the alveolar bone (AB). *Dspp* transcripts were also specifically present in odontoblasts. In higher magnification, the epithelial root sheath (ERT) is localized by immunohistochemistry using pan-keratin antibodies. Odontoblasts (od) are columnar cells lining the pulpal surface of dentin (de), and preodontoblasts (pod) are the odontoblast precursors in the apical end of the root. At the apical end of the growing root, *Wnt10a* transcripts were present in the preodontoblasts (pod). (**D**) The expression was continuous and maintained in differentiating and secretory odontoblasts (od). (**E**) *Dspp* expression was only detected in polarized odontoblasts (od). en, enamel; PDL, periodontal ligament. (**F**) Strong *Bmp3* expression was detected in cementoblasts the 1st and 2nd molars, as well as the dental follicle around all three molars. It was also observed in the osteoblasts on the active bone-forming surface.

using pan-keratin antibodies (Fig. 1C). Odontoblasts can be visualized as columnar cells lining the pulpal surface of dentin, and as the gradient of cell differentiation extends towards the root apex, preodontoblasts, i.e. the odontoblast precursors are present next to the root sheath (Fig. 1C). In higher magnification, *Wnt10a* transcripts were detected in differentiating and secretory odontoblasts and they were also diffusely present in the preodontoblasts underlying the epithelial root sheath (Fig. 1D). Previous reports showed that *Dspp* expres-

sion is initiated with matrix mineralization. *Dspp* was present in polarized odontoblasts but absent in pre-odontoblasts and differentiating odontoblasts indicating that the expression of *Wnt10a* precedes *Dspp* during the differentiation of the odontoblast cell lineage (Fig. 1E). At this stage, osteogenesis and cementogenesis were also active, as shown by intense *Bmp3* signals on the surfaces of bone and cementum (Fig. 1F) (Yamashiro et al., 2002). Hence, *Wnt10a* expression was expressed specifically in secretory odontoblasts

Wnt10a overexpression induces *Dspp* expression

As *Wnt10a* and *Dspp* transcripts overlapped in the odontoblasts but *Wnt10a* appeared earlier than *Dspp* in the odontoblast cell lineage, we hypothesized that Dspp might be induced by Wnt10a. To test this possibility, we overexpressed *Wnt10a* in the C310T1/2 cell line and examined its effect on *Dspp* expression. RT-PCR confirmed that C310T1/2 cells and Mock-transfected cells did not express *Wnt10a* mRNA, whereas *Wnt10a* transfected cells at 24 hr post-transfection and the cells derived from P1 tooth germs showed 340-bp bands of *Wnt10a* (Fig. 2A).

Induction of *Dspp* expression was detected in the *Wnt10a* transfected cells by real-time PCR ten days after transfection, but not after five or fifteen days. C3H10T1/2 cells did not show *Dspp* expression (Figs. 3A,3B). Gel electrophoresis of RT-PCR products (40 cycles) demonstrate a single band of 550 bp, corresponding to the *Dspp* transcript in cDNA derived from total RNA obtained from C310T1/2 cells transfected with pCMV-Wnt10a and cultured on Matrigel (Wnt10a Mg(+)), and positive control (tooth germ; Fig. 3B), indicating that *Dspp* induction was seen only when the cells were cultured on Matrigel coated dishes. Matrigel is an extract of basement membrane proteins (Kleinman et al., 1982 #16), and *Wnt10a* transfected cells cultured on conventional collagen coated dishes did not express *Dspp*. Mock transfected cells cultured on Matrigel dishes did not show *Dspp* expression (Figs. 3A,3B), indicating that Matrigel itself did not induce *Dspp*. These results indicated that Wnt10 can induce *Dspp* expression and that the specific basement membrane matrix was essential for this induction.

We confirmed the specificity of the amplified products and PCR products were not detected in Mock-transfected cells. The integrity of the RT-PCR products was confirmed by melting curve analysis (Fig. 3C). Melting curve analysis showed that the Tm of the *Dspp* templates was 88.5°C and occurred as a single amplicon peak for both *Wnt10a* transfected cells and control samples, reflecting the specificity of the PCR-products (Fig. 3C). The non-specific products, such as primer dimers, sometimes appeared, however, they melt below 80°C and were differentiated from the specific products by the melting curve analysis. These results were also

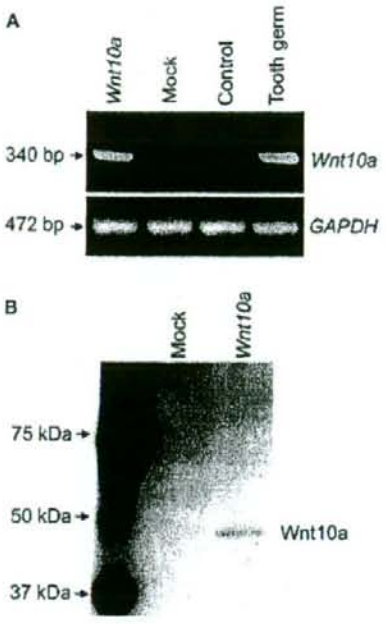

Fig. 2 C310T1/2 cells were transiently transfected with expression vectors encoding *Wnt10a*. (**A**) Expression of *Wnt10a* mRNA in C310T1/2 cells. After 24 hr transient transfection, total mRNA was extracted and submitted to reverse-transcriptase polymerase chain reaction (RT-PCR) using oligonucleotide primers specific of *Wnt10a* and *GAPDH*. Cells were transfected with pCMV-Wnt10a (Wnt10a) or its vehicle pCMV (Mock). Total RNA was also isolated from tooth germs and used as a positive control (tooth germ, 30 cycles). Negative control (control, 30 cycles) was performed in the absence of oligonucleotides. RT-PCR confirmed transfection efficiency using pCMV-WNT10a (Wnt10a, 30 cycles). (**B**) Expression of Wnt10a protein in C310T1/2 cells. Overexpression of Wnt10a protein was also confirmed by Western blot analysis 48 hr after transfection. Cells were lysed in sodium dodecyl sulfate-polyacrylamide gel electrophoresis (SDS-PAGE) loading buffer after transfection and analyzed by Western blot with specific antibodies to Wnt10a. pCMV-Wnt10-transfected (Wnt10a) cells showed Wnt10a protein expression. This protein expression was not observed in control cells transfected with vehicle pCMV (Mock). A molecular weight marker was run in parallel in the first lane.

confirmed by gel electrophoresis. Transfection and PCR were repeated three times.

Expression of *Wnt10a* during tooth development

At E14, the cap stage of tooth development, *Wnt10a* transcripts were intensely expressed in the enamel knot, as shown previously (Dassule and McMahon, 1998). No *Wnt10a* expression was detected in the dental mesenchyme (Fig. 4A). At E16, early bell stage, the primary enamel knot had disappeared, and *Wnt10a* was detected in secondary enamel knots. In addition, the mesenchymal cells directly underlying the enamel knots expressed *Wnt10a* (Fig. 4B). Subsequently at E18 transcripts were

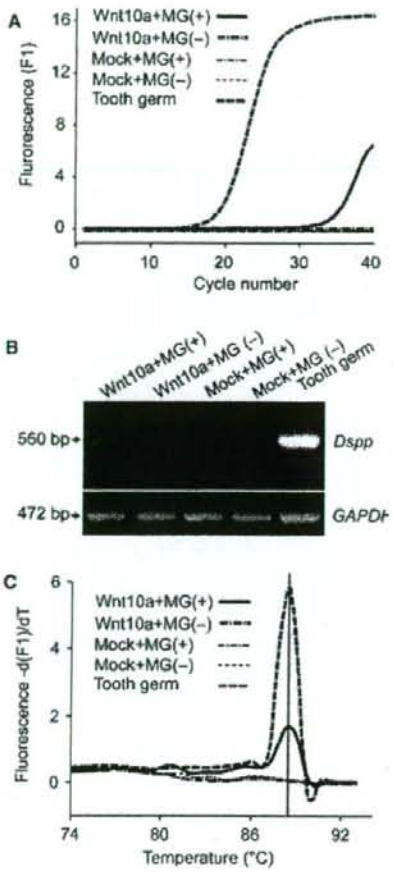

Fig. 3 Wnt10a transient transfection in C310T1/2 cells induced dentin sialophosphoprotein (Dspp) gene expression. (**A**) C310T1/2 cells were transiently transfected with pCMV-Wnt10a (Wnt10a) or its vehicle pCMV (Mock). Transfected cells were harvested 10 day post-transfection on Matrigel (Mg (+)) or collagen coated dishes (Mg (−)). Total mRNA extracted from the transfected cells was reverse transcribed and submitted to real-time polymerase chain reaction (PCR) using oligonucleotide primers specific of Dspp. Total RNA was also isolated from tooth germs and used as a positive control (Tooth germ). The *x*-axis denotes the cycle number of a quantitative PCR assay, and the y axis denotes the fluorescence intensity (F1) over the background. Amplification of Dspp was observed in C310T1/2 cells transfected with pCMV-Wnt10a and cultured on Matrigel (Wnt10a+Mg (+)), and positive control (tooth germ). (**B**) Forced-expression of Wnt10a induced Dspp expression when the transfected cells were cultured on Matrigel dishes (Wnt10a+Mg (+), 40 cycles). Wnt10a transfected cells cultured on normal culture dishes (Wnt10a+Mg (−), 40 cycles) and Mock transfected cells cultured on Matrigel dishes (Mock+Mg (+), 40 cycles) or normal culture dishes (Mock+Mg (−), 40 cycles) did not show Dspp expression. Positive control (Tooth germ) showed intense Dspp expression. (**C**) PCR products were subjected to melting peak analyses to determine the specificity of the products. Dspp sample showed a single product with Tm values of 88.5°C.

accumulated in the single cell layer of differentiating odontoblasts, which were aligned under the basement membrane (Fig. 4C). At E18, the differentiating odontoblasts became polarized and odontoblast differentiation initiated from the tips of the future cusps where the enamel knots are located (Fig. 5A). As the differentiation of preodontoblasts proceeded from the cusp tips in cervical direction along the cusp slopes *Wnt10a* expression was intimately linked with this gradient of differentiation. (Fig. 5B), and was highest in the cusp regions (Fig. 5C). *Dspp* expression was not yet expressed in the odontoblast lineage at this stage (Bleicher et al., 1999). In the early osteogenesis, *Wnt10a* was detected in the future bone regions at E13 and E14 (data not shown). This expression was down-regulated significantly at E16 and the expression could not be detected at P14 (Fig. 1A).

Discussion

The expression pattern of *Wnt10a* is associated with odontoblast differentiation

Our *in situ* hybridization analysis revealed that the expression of *Wnt10a* mRNA was associated with dentinogenesis. We found that *Wnt10a* expression was intense in the odontoblast cell layer and that it was maintained specifically in secretory odontoblasts where it was coexpressed with *Dspp*. In root development stage, mineralized matrix is also actively formed on the surface of bone and cementum, and the distribution of *Bmp3* expression indicated the regions of active osteogenesis and cementogenesis at the root surface and the surrounding alveolar bone surface. The comparison of *Wnt10a* and *Bmp3* distribution revealed that *Wnt10a* expression was specifically involved in odontogenesis, but not in osteogenesis or cementogenesis.

At the tip of the growing root, Hertwig's epithelial root sheath proliferates and directs root morphogenesis. The pulpal mesenchyme provides precursors for odontoblasts, and the subpopulation of pulp cells that contact the epithelial root sheath differentiate into preodontoblasts. As odontoblast differentiation is characterized by cytological polarization and they are lining in one cell layer they can be clearly distinguished from the surrounding pulpal cells. *In situ* hybridization analysis demonstrated that *Wnt10a* was not expressed in the pulpal mesenchyme, indicating that Wnt10a is induced when the precursor cells start to differentiate into odontoblasts.

Wnt10a regulates the expression of *Dspp*

Dspp and *Wnt10a* were colocalized in the differentiated odontoblasts. However, at the tip of the growing root,

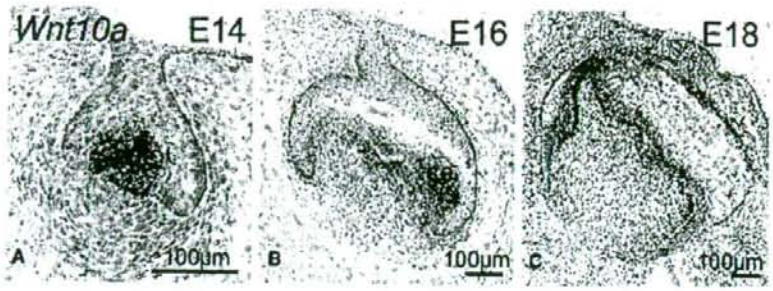

Fig. 4 At E14 (cap stage) *Wnt10a* transcripts were present in the primary enamel knot (pe), as shown previously. No expression was detected in the dental mesenchyme (**A**). At E16 (early bell stage) *Wnt10a* was detected in secondary enamel knots (se). In addition gene expression had shifted to the underlying mesenchymal cells (**B**). At E18 transcripts were accumulated in the single cell layer of differentiating odontoblasts (**C**).

Wnt10a expression was present in preodontoblasts beneath the epithelial sheath, but *Dspp* expression was absent indicating that *Wnt10a* expression appeared earlier than *Dspp* expression. Similarly, in early tooth development *Wnt10a* expression was first initiated in the odontogenic lineage cells at E14 whereas *Dspp* appeared in odontoblasts at E17 (Yamazaki et al., 1999). This temporo-spatial distribution pattern was in line with the possibility of an inductive role of *Wnt10a* on *Dspp* expression and we confirmed by transient overexpression of *Wnt10a* in C310T1/2 cells that Dspp was downstream of Wnt10a. The C310T1/2 cell line is derived from embryonic mesodermal cells, and can differentiate into distinctly different cell lineages, myoblasts, adipocytes, chondrocytes and osteoblasts under the influence of certain inducers (Taylor and Jones, 1979; Katagiri et al., 1990; Asahina et al., 1996). As C31010T1/2 cells did not constitutively express either *Wnt10a* or *Dspp* mRNA, our data indicated that *Dspp* was induced by Wnt10a in C31010T1/2 cells and that it may be a direct downstream target of Wnt10a (Fig. 6).

The extracellular mineralizing matrices of dentin and bone share many similarities, and it is likely that regulation of osteoblast and odontoblast differentiation may involve same signaling molecules (Thesleff et al., 2001). To our knowledge, Wnt10a is the first signal molecule that has specifically associated with odontoblast differentiation. Various Wnt genes, such as *Wnt1*, *Wnt4*, *Wnt5a*, *Wnt9a/14* and *Wnt7b*, are expressed in either osteoblast precursors or adjacent tissues during embryonic development, and *Wnt3a* and *Wnt10b* are expressed in bone marrow (Hartmann, 2006). In our study, we also demonstrated that *Wnt10a* was expressed in the future bone regions, but its expression was not maintained in the postnatal bone. Among these Wnt molecules, *Wnt10b* mutants display a postnatal decrease in bone mass and serum osteocalcin level, indicating that Wnt10b is an endogenous regulator of bone formation (Bennett et al., 2005). Wnt10b is homologous to Wnt10a, and WNT6 and WNT10a genes are clustered in tail-to-head manner. Like *Wnt10a*, both *Wnt10b* and *Wnt6* are expressed in the enamel knot and the dental epithelium in early tooth development (Dassule and McMahon, 1998; Sarkar and Sharpe, 1999). However, during later tooth development, *Wnt6* or *Wnt10b* transcripts were not detected in the odontoblast cell lineage by *in situ* hybridization (data not shown).

Cell to matrix interactions are required for the induction of *Dspp* expression by Wnta10a

Studies in the 1970's and 1980's showed that odontoblast differentiation depends on contacts between the

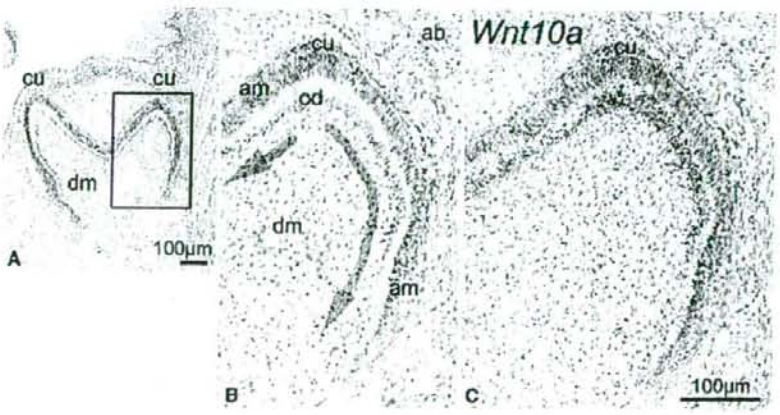

Fig. 5 Coronal sections of E18 molar (late bell stage) (**A**). (**B**) Higher magnification of the labial half of 1st molar (inset in panel A). Odontoblast differentiation has initiated beneath the forming cusp (cu) and the cells have polarized. (**C**). Wnt10a expression is associated with the gradient of odontoblast cytodifferentiation, and is highest in the cusp regions (cu).

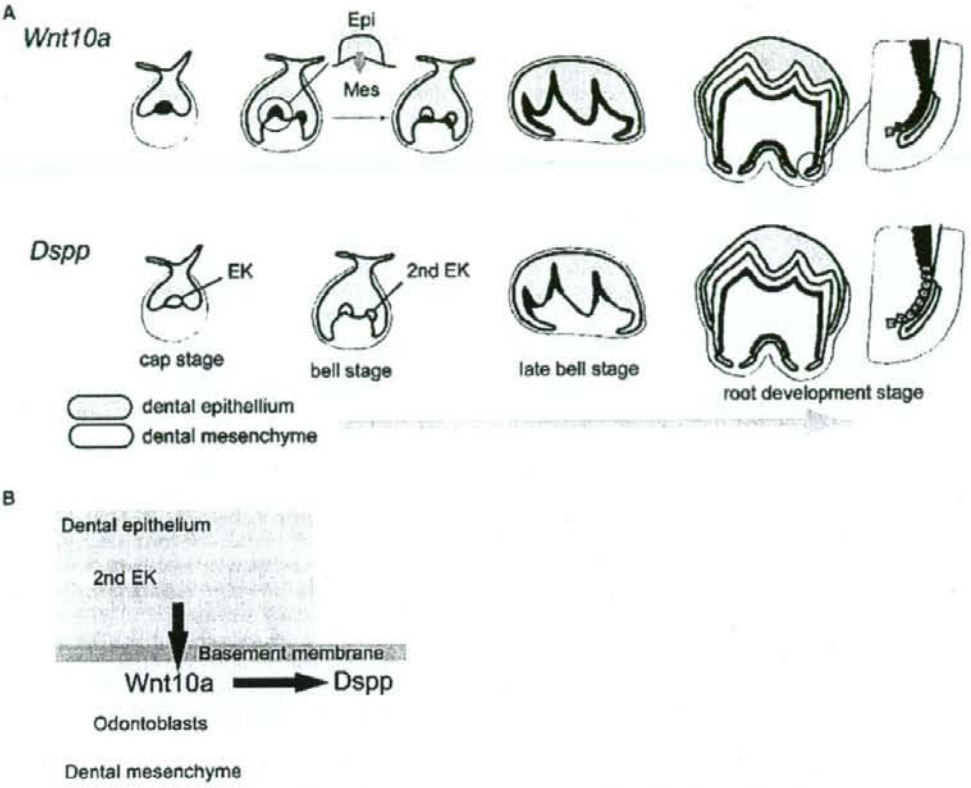

Fig. 6 (A) Summary of the expression of *Wnt10a* and *Dspp* during tooth development. *Wnt10a* is expressed in the enamel knot (EK) at the cap stage. At the bell stage, *Wnt10a* is expressed in the secondary enamel knot (2nd EK), and the expression has shifted to the underlying mesenchyme. In the late bell stages, *Wnt10a* expression is continuous in the preodontoblasts and odontoblasts. *Dspp* is expressed in the odontoblasts in the cusp regions. During root development, both *Wnt10a* and *Dspp* expression domains overlap in the odontoblasts. However, *Wnt10a* expression appeared earlier in the differentiating preodontoblasts underlying the epithelial root sheath. (B) Schematic diagram illustrating induction of *Dspp* expression by Wnt10a signals in the odontoblast cell lineage. *Wnt10a* appears in the mesenchymal cells beneath the secondary enamel knots. Wnt10a induces *Dspp* expression in the odontoblasts, and cell to matrix interactions are required for the induction of *Dspp* expression by Wnta10a. Hence, Wnt10a links tooth morphogenesis and odontoblast differentiation.

mesenchymal cells and the basement membrane underlining the enamel epithelium (Thesleff and Hurmerinta, 1981). Many extracellular matrix molecules were implicated in the cell–matrix interactions including fibronectin and other glycoproteins as well as proteoglycans. It was also suggested that growth factors and other diffusible molecules may have been trapped in the basement membrane, and involved in communication between cells. Interestingly, *Dspp* was induced only when the *Wnt10a*-transfected cells were cultured on Matrigel, which is an extract of basement membrane proteins (Kleinman et al., 1982), supporting the idea that cell to matrix association plays some role in odontoblast differentiation. As Mock-transfected cell did not show *Dspp* expression on Matrigel, Matrigel itself cannot induce odontogenesis. Among various molecules in the basement membrane, laminin alfa2 is subunit of laminin-2. Laminin-α2 deficiency resulted in a dramatic decrease in *Dspp* expression in odontoblasts (Yuasa et al., 2004), which is in agreement with our data and also supports the idea that cell–matrix interaction is essential for Dspp expression.

Heparan sulfate proteoglycans are major components of the extracellular matrix and regulate the transmission of developmental signals (Hacker et al., 2005). They also modulate the Wnt pathway (Haerry et al., 1997). In tooth development, odontoblast differentiation was inhibited *in vitro* by tunicamycin, which inhibited protein glycosylation and the accumulation of proteoglycans and glycoproteins in the basement mem-

brane of the developing tooth (Thesleff and Pratt, 1980). In tooth development also the cell surface proteoglycan syndecan-1 is involved in epithelial–mesenchymal interactions (Vainio et al., 1989; Thesleff et al., 1991), and syndecan-3 has been detected in the odontoblast layer underlying the inner enamel epithelium (Hikake et al., 2003). Heparin-sulfated forms of proteoglycans (HSPG) are long proteins with branched sugar side chains that are expressed on the cell surface, and can form complexes with a variety of signaling molecules, including Wnts and fibroblast growth factors (Nybakken and Perrimon, 2002). Hence it is possible that Wnt10a can be captured in the basement membrane extracellular matrix molecules to control differentiation of the pulp cells into odontoblasts. In addition, spatial distribution patterns of *Wnt10a* mRNA expression, together with previous findings, might provide an insight into a possible association between Wnt signaling and heparan sulfate proteoglycan in dentinogenesis. With tooth development, the basement membrane degrades and odontoblasts come into contact with the predentin surface. As predentin also contains various extracellular matrix molecules, such as proteoglycan and fibronectin (Linde and Goldberg, 1993), the cell–matrix interaction between odontoblasts and predentin might thus be explained the continuous expression of Wnt10a and Dspp in odontoblasts after the basement membrane has disappeared.

In our study, transfected cells were cultured on Matrigel in the medium supplemented with serum. Although both serum and Matrigel contain many growth factors and proteins these did not induce odontoblast differentiation as shown by the lack of *Dspp* expression in Mock transfected cells. Our real-time PCR data demonstrated that the *Dspp* induction by forced overexpression of *Wnt10a* was specific.

Odontoblast differentiation is regulated by reciprocal epithelial mesenchymal interactions. In addition, Dspp is expressed in a time- and site-specific manner and Dspp-expressing odontoblasts lie in one cell layer. These findings suggest that Dspp expression could be regulated by several inhibitory and stimulatory factors in a coordinated manner. Our real-time PCR data showed that Dspp induction in Wnt10a transfected-non-odontogenic cells was much less than the Dspp expression in intact odontoblasts. These data suggested that Wnt10a thus plays an important role in Dspp induction, however, further interaction with other putative molecules might be necessary to express a sufficient amount of Dspp during odontoblast differentiation.

Wnt10a and tooth morphogenesis

In the early tooth, *Wnt10a* is expressed in the enamel knot (Dassule and McMahon, 1998), which has a central function in the control of growth and patterning of the tooth crown (Jernvall and Thesleff, 2000; Miletich and Sharpe, 2003). Our *in situ* hybridization analysis showed that *Wnt10a* expression was reiterated in the secondary enamel knots which express most of the same signal molecules as the primary enamel knots and initiate cusp formation (Fig. 6A) (Vaahtokari et al., 1996). Interestingly, we found that *Wnt10a* expression shifted from the secondary enamel knots to the underlying mesenchyme. It could be that mesenchymal *Wnt10a* expression was induced by signaling molecules of the secondary enamel knots, perhaps by Wnt10a itself. The continuous *Wnt10a* mRNA distribution pattern in the odontoblasts suggested autocrine regulation of *Wnt10a* expression in the mesenchymal cells after the initial induction of *Wnt10a* by the epithelium.

Our study has provided new insight into the molecular mechanisms that spatially and temporally control the initiation of odontoblast differentiation. The terminal differentiation of odontoblasts is initiated at the tip of each cusp, indicating that the cell fate decision and morphogenesis is tightly linked (Fig. 6B). As both the initiation of odontoblast differentiation and the initiation of cusps coincide temporally and spatially with the secondary enamel knots, and as both processes are induced by epithelial signals (Jernvall et al., 1994; Jernvall and Thesleff, 2000), it is conceivable that some signals could regulate both cell differentiation as cusp morphogenesis. Our observations indicated that the expression of Wnt10a was intimately linked with the secondary enamel knots and the gradient of cytodifferentiation propagating apically from each cusp tip. Our data clearly demonstrated that *Wnt10a*-shifting from the epithelial signaling center to the underlying mesenchyme temporally and spatially corresponds to the initiation of odontoblast differentiation. In addition, functional network of Wnt10a and the cell to matrix interactions may trigger and regulate tooth specific *Dspp* expression. Putative matrix molecules may provide the cues for polarization of the cells, which may be necessary also for the transmission of the Wnt10a signal from the epithelium to the preodontoblast.

In summary, we found that *Wnt10a* was specifically expressed in the odontoblast cell lineage in mouse molars with striking colocalization with *Dspp* mRNA expression in the fully differentiated secretory odontoblasts. Dspp is a key molecule for dentin mineralization, and we showed that the forced expression of *Wnt10a* induced *Dspp* mRNA in pluripotent fibroblast cells, indicating that Wnt10a is possibly involved in dentine mineralization as an upstream regulator of Dspp. However, our observation that *Dspp* was induced only when the transfected cells were cultured on Matrigel suggests that cell to matrix interactions have crucial roles in dentinogenesis in conjunction with Wnt10a. This supports earlier proposals that odontoblast differentiation requires interactions between the mesenchymal cells and the extracellular matrix. We also found

that *Wnt10a* was expressed in the epithelial secondary enamel knots, and that this expression shifted to the underlying mesenchymal cells. The timing and location of this shift corresponds to the initiation of the polarization of preodontoblasts. Taken together, our findings indicate that Wnt10a and cell to matrix interactions play an important role for odontoblast differentiation and that Wnt10a links tooth morphogenesis and the differentiation of odontoblasts.

Acknowledgments We thank Merja Mäkinen and Riikka Santalahti for their excellent technical assistance. This study was supported by Grants-in-Aid for Scientific Research from the Japan Society for the Promotion of Science, the Academy of Finland, and the Sigrid Juselius Foundation.

References

Åberg, T., Wozney, J. and Thesleff, I. (1997) Expression patterns of bone morphogenetic proteins (Bmps) in the developing mouse tooth suggest roles in morphogenesis and cell differentiation. Dev Dyn 210:383–396.

Asahina, I., Sampath, T.K. and Hauschka, P.V. (1996) Human osteogenic protein-1 induces chondroblastic, osteoblastic, and/or adipocytic differentiation of clonal murine target cells. Exp Cell Res 222:38–47.

Bennett, C.N., Longo, K.A., Wright, W.S., Suva, L.J., Lane, T.F., Hankenson, K.D. and MacDougald, O.A. (2005) Regulation of osteoblastogenesis and bone mass by Wnt10b. Proc Natl Acad Sci USA 102:3324–3329.

Bleicher, F., Couble, M.L., Farges, J.C., Couble, P. and Magloire, H. (1999) Sequential expression of matrix protein genes in developing rat teeth. Matrix Biol 18:133–143.

Cadigan, K.M. and Nusse, R. (1997) Wnt signaling: a common theme in animal development. Genes Dev 11:3286–3305.

Dassule, H.R. and McMahon, A.P. (1998) Analysis of epithelial–mesenchymal interactions in the initial morphogenesis of the mammalian tooth. Dev Biol 202:215–227.

D'Souza, R.N., Cavender, A., Sunavala, G., Alvarez, J., Ohshima, T., Kulkarni, A.B. and MacDougall, M. (1997) Gene expression patterns of murine dentin matrix protein 1 (Dmp1) and dentin sialophosphoprotein (DSPP) suggest distinct developmental functions in vivo. J Bone Miner Res 12:2040–2049.

Feng, J.Q., Luan, X., Wallace, J., Jing, D., Ohshima, T., Kulkarni, A.B., D'Souza, R.N., Kozak, C.A. and MacDougall, M. (1998) Genomic organization, chromosomal mapping, and promoter analysis of the mouse dentin sialophosphoprotein (Dspp) gene, which codes for both dentin sialoprotein and dentin phosphoprotein. J Biol Chem 273:9457–9464.

Hacker, U., Nybakken, K. and Perrimon, N. (2005) Heparan sulphate proteoglycans: the sweet side of development. Nat Rev Mol Cell Biol 6:530–541.

Haerry, T.E., Heslip, T.R., Marsh, J.L. and O'Connor, M.B. (1997) Defects in glucuronate biosynthesis disrupt Wingless signaling in Drosophila. Development 124:3055–3064.

Hartmann, C. (2006) A Wnt canon orchestrating osteoblastogenesis. Trends Cell Biol 16:151–158.

Hikake, T., Mori, T., Iseki, K., Hagino, S., Zhang, Y., Takagi, H., Yokoya, S. and Wanaka, A. (2003) Comparison of expression patterns between CREB family transcription factor OASIS and proteoglycan core protein genes during murine tooth development. Anat Embryol (Berlin) 206:373–380.

James, M.J., Jarvinen, E. and Thesleff, I. (2004) Bonol: a gene associated with regions of deposition of bone and dentine. Gene Expr Patterns 4:595–599.

Jernvall, J., Kettunen, P., Karavanova, I., Martin, L.B. and Thesleff, I. (1994) Evidence for the role of the enamel knot as a control center in mammalian tooth cusp formation: non-dividing cells express growth stimulating Fgf-4 gene. Int J Dev Biol 38:463–469.

Jernvall, J. and Thesleff, I. (2000) Reiterative signaling and patterning during mammalian tooth morphogenesis. Mech Dev 92:19–29.

Katagiri, T., Yamaguchi, A., Ikeda, T., Yoshiki, S., Wozney, J.M., Rosen, V., Wang, E.A., Tanaka, H., Omura, S. and Suda, T. (1990) The non-osteogenic mouse pluripotent cell line, C3H10T1/2, is induced to differentiate into osteoblastic cells by recombinant human bone morphogenetic protein-2. Biochem Biophys Res Commun 172:295–299.

Kleinman, H.K., McGarvey, M.L., Liotta, L.A., Robey, P.G., Tryggvason, K. and Martin, G.R. (1982) Isolation and characterization of type IV procollagen, laminin, and heparan sulfate proteoglycan from the EHS sarcoma. Biochemistry 21: 6188–6193.

Kollar, E.J. (1985) Tissue interactions in development of teeth and related ectodermal derivatives. Dev Biol (NewYork) 4: 297–313.

Kratochwil, K., Galceran, J., Tontsch, S., Roth, W. and Grosschedl, R. (2002) FGF4, a direct target of LEF1 and Wnt signaling, can rescue the arrest of tooth organogenesis in Lef1(−/−) mice. Genes Dev 16:3173–3185.

Lesot, H., Lisi, S., Peterkova, R., Peterka, M., Mitolo, V. and Ruch, J.V. (2001) Epigenetic signals during odontoblast differentiation. Adv Dent Res 15:8–13.

Linde, A. and Goldberg, M. (1993) Dentinogenesis. Crit Rev Oral Biol Med 4:679–728.

Miletich, I. and Sharpe, P.T. (2003) Normal and abnormal dental development. Hum Mol Genet 12(Spec No 1): R69–R73.

Nakashima, M., Nagasawa, H., Yamada, Y. and Reddi, A.H. (1994) Regulatory role of transforming growth factor-beta, bone morphogenetic protein-2, and protein-4 on gene expression of extracellular matrix proteins and differentiation of dental pulp cells. Dev Biol 162:18–28.

Nusse, R. (2003) Wnts and Hedgehogs: lipid-modified proteins and similarities in signaling mechanisms at the cell surface. Development 130:5297–5305.

Nybakken, K. and Perrimon, N. (2002) Heparan sulfate proteoglycan modulation of developmental signaling in Drosophila. Biochim Biophys Acta 1573:280–291.

Qin, C., Brunn, J.C., Cadena, E., Ridall, A., Tsujigiwa, H., Nagatsuka, H., Nagai, N. and Butler, W.T. (2002) The expression of dentin sialophosphoprotein gene in bone. J Dent Res 81:392–394.

Rajpar, M.H., Koch, M.J., Davies, R.M., Mellody, K.T., Kielty, C.M. and Dixon, M.J. (2002) Mutation of the signal peptide region of the bicistronic gene DSPP affects translocation to the endoplasmic reticulum and results in defective dentine biomineralization. Hum Mol Genet 11:2559–2565.

Ruch, J.V., Lesot, H., Karcher-Djuricic, V., Meyer, J.M. and Olive, M. (1982) Facts and hypotheses concerning the control of odontoblast differentiation. Differentiation 21:7–12.

Sarkar, L. and Sharpe, P.T. (1999) Expression of Wnt signalling pathway genes during tooth development. Mech Dev 85:197–200.

Shiba, H., Fujita, T., Doi, N., Nakamura, S., Nakanishi, K., Takemoto, T., Hino, T., Noshiro, M., Kawamoto, T., Kurihara, H. and Kato, Y. (1998) Differential effects of various growth factors and cytokines on the syntheses of DNA, type I collagen, laminin, fibronectin, osteonectin/secreted protein, acidic and rich in cysteine (SPARC), and alkaline phosphatase by human pulp cells in culture. J Cell Physiol 174:194–205.

Shields, E.D., Bixler, D. and el-Kafrawy, A.M. (1973) A proposed classification for heritable human dentine defects with a description of a new entity. Arch Oral Biol 18:543–553.

Sreenath, T., Thyagarajan, T., Hall, B., Longenecker, G., D'Souza, R., Hong, S., Wright, J.T., MacDougall, M., Sauk, J. and

Kulkarni, A.B. (2003) Dentin sialophosphoprotein knockout mouse teeth display widened predentin zone and develop defective dentin mineralization similar to human dentinogenesis imperfecta type III. J Biol Chem 278:24874–24880.

Taylor, S.M. and Jones, P.A. (1979) Multiple new phenotypes induced in 10T1/2 and 3T3 cells treated with 5-azacytidine. Cell 17:771–779.

Thesleff, I. and Aberg, T. (1999) Molecular regulation of tooth development. Bone 25:123–125.

Thesleff, I. and Hurmerinta, K. (1981) Tissue interactions in tooth development. Differentiation 18:75–88.

Thesleff, I. and Pratt, R.M. (1980) Tunicamycin inhibits mouse tooth morphogenesis and odontoblast differentiation in vitro. J Embryol Exp Morphol 58:195–208.

Thesleff, I., Keranen, S. and Jernvall, J. (2001) Enamel knots as signaling centers linking tooth morphogenesis and odontoblast differentiation. Adv Dent Res 15:14–18.

Thesleff, I., Partanen, A.M. and Vainio, S. (1991) Epithelial–mesenchymal interactions in tooth morphogenesis: the roles of extracellular matrix, growth factors, and cell surface receptors. J Craniofac Genet Dev Biol 11:229–237.

Thesleff, I., Vainio, S. and Jalkanen, M. (1989) Cell–matrix interactions in tooth development. Int J Dev Biol 33:91–97.

Tsukamoto, Y., Fukutani, S., Shin-Ike, T., Kubota, T., Sato, S., Suzuki, Y. and Mori, M. (1992) Mineralized nodule formation by cultures of human dental pulp-derived fibroblasts. Arch Oral Biol 37:1045–1055.

Vaahtokari, A., Aberg, T., Jernvall, J., Keranen, S. and Thesleff, I. (1996) The enamel knot as a signaling center in the developing mouse tooth. Mech Dev 54:39–43.

Vainio, S., Jalkanen, M. and Thesleff, I. (1989) Syndecan and tenascin expression is induced by epithelial–mesenchymal interactions in embryonic tooth mesenchyme. J Cell Biol 108: 1945–1953.

Vainio, S., Karavanova, I., Jowett, A. and Thesleff, I. (1993) Identification of BMP-4 as a signal mediating secondary induction between epithelial and mesenchymal tissues during early tooth development. Cell 75:45–58.

van Genderen, C., Okamura, R.M., Farinas, I., Quo, R.G., Parslow, T.G., Bruhn, L. and Grosschedl, R. (1994) Development of several organs that require inductive epithelial–mesenchymal interactions is impaired in LEF-1-deficient mice. Genes Dev 8:2691–2703.

Wang, J. and Shackleford, G.M. (1996) Murine Wnt10a and Wnt10b: cloning and expression in developing limbs, face and skin of embryos and in adults. Oncogene 13:1537–1544.

Xiao, S., Yu, C., Chou, X., Yuan, W., Wang, Y., Bu, L., Fu, G., Qian, M., Yang, J., Shi, Y., Hu, L., Han, B., Wang, Z., Huang, W., Liu, J., Chen, Z., Zhao, G. and Kong, X. (2001) Dentinogenesis imperfecta 1 with or without progressive hearing loss is associated with distinct mutations in DSPP. Nat Genet 27: 201–204.

Yamashiro, T., Tummers, M. and Thesleff, I. (2003) Expression of bone morphogenetic proteins and Msx genes during root formation. J Dent Res 82:172–176.

Yamazaki, H., Kunisada, T., Miyamoto, A., Tagaya, H. and Hayashi, S. (1999) Tooth-specific expression conferred by the regulatory sequences of rat dentin sialoprotein gene in transgenic mice. Biochem Biophys Res Commun 260:433–440.

Yuasa, K., Fukumoto, S., Kamasaki, Y., Yamada, A., Fukumoto, E., Kanaoka, K., Saito, K., Harada, H., Arikawa-Hirasawa, E., Miyagoe-Suzuki, Y., Takeda, S., Okamoto, K., Kato, Y. and Fujiwara, T. (2004) Laminin alpha2 is essential for odontoblast differentiation regulating dentin sialoprotein expression. J Biol Chem 279:10286–10292.

Zhang, X., Zhao, J., Li, C., Gao, S., Qiu, C., Liu, P., Wu, G., Qiang, B., Lo, W.H. and Shen, Y. (2001) DSPP mutation in dentinogenesis imperfecta Shields type II. Nat Genet 27:151–152.

Cell Tissue Res
DOI 10.1007/s00441-006-0257-6

REGULAR ARTICLE

Establishment of immortalized dental follicle cells for generating periodontal ligament in vivo

T. Yokoi · M. Saito · T. Kiyono · S. Iseki · K. Kosaka · E. Nishida · T. Tsubakimoto · H. Harada · K. Eto · T. Noguchi · T. Teranaka

Received: 23 January 2006 / Accepted: 24 May 2006

Abstract The dental follicle is a mesenchymal tissue that surrounds the developing tooth germ. During tooth root formation, periodontal components, viz., cementum, periodontal ligament (PDL), and alveolar bone, are created by dental follicle progenitors. Here, we report the presence of PDL progenitors in mouse dental follicle (MDF) cells. MDF cells were obtained from mouse incisor tooth germs and immortalized by the expression of a mutant human papilloma virus type 16 *E6* gene lacking the PDZ-domain-binding motif. MDF cells expressing the mutant *E6* gene ($MDF^{E6\text{-}EGFP}$ cells) had an extended life span, beyond 150 population doublings (PD). In contrast, normal MDF cells failed to proliferate beyond 10 PD. $MDF^{E6\text{-}EGFP}$ cells expressed tendon/ligament phenotype-related genes such as *Scleraxis* (*Scx*), *growth and differentiation factor-5*, *EphA4*, *Six-1*, and *type I collagen*. In addition, the expression of *periostin* was observed. To elucidate the differentiation capacity of $MDF^{E6\text{-}EGFP}$ cells in vivo, the cells were transplanted into severe combined immunodeficiency mice. At 4 weeks, $MDF^{E6\text{-}EGFP}$ cell transplants had the capacity to generate a PDL-like tissue that expressed *periostin*, *Scx*, and *type XII collagen* and the fibrillar assembly of type I collagen. Our findings suggest that $MDF^{E6\text{-}EGFP}$ cells can act as PDL progenitors, and that these cells may be a useful research tool for studying PDL formation and for developing regeneration therapies.

Keywords Dental follicle · Progenitor · Development · Immortalization · Periodontal ligament · Mouse (ICR)

This work was supported by a Grant-in Aid for the High-Tech Research Center Project from the Ministry of Education, Culture, Sports, Science, and Technology of Japan, the AGU High-Tech Research Center Project, the 2003-Multidisciplinary Research Project from MEXT, and grants from the Ministry of Education, Culture, Sports, Science, and Technology of Japan.

T. Yokoi · M. Saito (✉) · K. Kosaka · E. Nishida · T. Tsubakimoto · T. Teranaka
Department of Medicine,
Division of Operative Dentistry and Endodontics,
Kanagawa Dental College,
82 Inaoka-cho,
Yokosuka, Kanagawa 238-8580, Japan
e-mail: saitohms@kdcnet.ac.jp

T. Yokoi · E. Nishida · T. Noguchi
Department of Periodontology, School of Dentistry,
Aichi-gakuin University,
Nagoya, Aichi, Japan

M. Saito
Oral Health Science Research Center, Kanagawa Dental College,
Yokosuka, Kanagawa, Japan

T. Kiyono
Virology Division, National Cancer Research Institute,
Tokyo, Japan

S. Iseki · K. Eto
Department of Molecular Craniofacial Embryology,
Graduate School, Tokyo Medical and Dental University,
Tokyo, Japan

H. Harada
Department of Oral Anatomy and Developmental Biology,
Osaka University Graduate School of Dentistry,
Suita, Osaka, Japan

Introduction

The periodontal ligament (PDL), which surrounds the tooth root, absorbs occlusal forces and functions as a sense organ (Ten Cate 1994). In periodontitis, a chronic inflammatory disease, the PDL is irreversibly damaged. Despite a number of novel approaches, no one has yet succeeded in reliably forming PDL (D'Errico et al. 1999).

Hence, there is considerable interest in the developmental mechanisms of PDL.

The PDL originates from dental follicle cells formed during the cap stage of tooth germ development by an ectomesenchymal progenitor cell population originating from cranial neural crest cells (Chai et al. 2000). Progenitors in the dental follicle are thought to contribute to the formation of all periodontal tissues, namely cementum, PDL, and alveolar bone (Bosshardt and Schroeder 1996). After the formation of tooth root dentin, cementoblast progenitors in the dental follicle migrate onto the tooth root surface and differentiate into cementoblasts (Bosshardt and Schroeder 1996). Almost simultaneously, PDL progenitors within the dental follicle cells differentiate into PDL cells. Finally, both bone- and PDL-derived fibers coalesce in the PDL to form the intermediate plexus. Although a specific marker for PDL is not available, tendon/ligament phenotype-related genes are thought to be involved in the differentiation of PDL progenitors. Growth and differentiation factors (GDFs)-5, 6, and 7 are members of the bone morphogenetic protein family that regulate tendon/ligament formation (Wolfman et al. 1997) and have been shown to be expressed by both dental follicle and PDL cells (Morotome et al. 1998; Nakamura et al. 2003; Sena et al. 2003). Screlaxis (*Scx*), a basic helix-loop-helix transcription factor that serves as a tendon progenitor marker gene, has also been found to be expressed by PDL stem cells (Brent et al. 2003; Seo et al. 2004). Non-collagenous extracellular matrix has been shown to be involved in the formation of PDL (Matias et al. 2003). *Periostin* is a marker for preosteoblasts but is also found in the periosteum and PDL (Horiuchi et al. 1999). During tooth germ development, *periostin* is initially expressed in the dental follicle cells and is then restricted to postnatal PDL cells during tooth root formation (Kruzynska-Frejtag et al. 2004). *Periostin-/-* mice develop a periodontal-disease-like phenotype within 3 months of birth, suggesting that this protein plays a critical role in maintenance of the PDL (Rios et al. 2005). These findings suggest that both tendon/ligament phenotype-related genes and extracellular matrices, which are highly expressed in PDL, are involved in PDL formation and maintenance. However, details of the mechanisms involved in PDL formation are yet to be clarified, because of the scarcity of PDL progenitor culture systems.

Recently, we have demonstrated the presence of cementoblast progenitors in bovine dental follicle cells (Handa et al. 2002). A cementoblast progenitor cell line, designated as BCPb8, has the capacity to form PDL- and cementum-like tissue when transplanted into severe combine immunodeficiency (SCID) mice (Saito et al. 2005). Although BCPb8 is a clonal cell line useful for the study of dental follicle progenitors, the use of these cells derived from a bovine species is restricted, because the cDNA database is inadequate, and because antibodies are limited. Thus, little is known about the biological properties of dental follicle progenitors or the mechanisms that regulate their differentiation. Investigations directed at addressing these key questions are essential if we are to understand the developmental mechanisms of PDL. In this study, we have attempted to establish immortalized mouse dental follicle (MDF) cells for the study of progenitors in dental follicle cells.

Materials and methods

Tissue culture

MDF cells were isolated from the dental follicle tissue of the incisor tooth germs of 1-day postnatal (P1) ICR mice. Briefly, mouse dental follicle tissue was mechanically stripped from the lingual posterior region of mouse incisor and placed onto a 24 multi-well plate. The tissues were then incubated with α-minimum essential medium (α-MEM: Sigma, St. Louis, USA) containing 10% fetal bovine serum (FBS; BioWhittaker, Maryland, USA), 50 μg/ml ascorbic acid, 100 U/ml streptomycin and penicillin, in a humidified atmosphere of 5% CO_2 at 37°C. When the cells reached approximately 80% confluence, they were passaged with 0.25% trypsin/1 mM EDTA and maintained as MDF cells. These cells were plated into six wells at a density of 3×10^4 cells/ml, and the medium was changed every 2 days.

Infection of retrovirus constructs and establishment of $MDF^{E6\text{-}EGFP}$ cells

The construction of pCLXSN-$16E6^{\Delta146\text{-}151}$ and the production of LXSN-$16E6^{\Delta146\text{-}151}$ retrovirus have been described previously (Kyo et al. 2003). An aliquot of 1 ml producer cell culture fluid was added to MDF cells (passage 1) in the presence of polybrene (8 μg/ml), and the cells were subsequently selected in the presence of G418 (100 μg/ml). Transduced cells were maintained in the medium described above. Following infection with LXSN-$16E6^{\Delta146\text{-}151}$, MDF cells were transduced with EGFP lentivirus under the control of a CMV promoter to obtain stably expressed EGFP ($MDF^{E6\text{-}EGFP}$).

Osteogenic differentiation

Cells were plated into six wells at a density of 3×10^4 cells/ml and cultured in the medium described above supplemented with 100 nM dexamethasone, 50 μg/ml ascorbic acid, 10 mM β-glycerophosphate. The culture medium was

replaced every 2 days, and the cells were maintained for 3 weeks.

Alkaline phosphatase activity and alizarin red staining

To evaluate alkaline phosphatase (ALP) activity, $MDF^{E6\text{-}EGFP}$ cells were fixed with 4% paraformaldehyde for 20 min at 21°C. After being washed with PBS, the cells were incubated for 20 min in a mixture of 0.1 mg/ml naphthol AS-MX phosphate (Sigma), 0.5% N-N dimethyl formamide (Sigma), 2 mM $MgCl_2$, 0.6 mg/ml Fast Blue BB salt (Sigma) in 0.1 M TRIS-HCl (pH 8.5) at room temperature. Calcium accumulation was detected by staining preparations with 2% alizarin red S (pH 6.4) (Sigma). MC3T3E1 (purchased from RIKEN BioResource Center, Japan) and NIH3T3 were used as controls.

Probes for in situ hybridization

The cDNA of mouse *osteopontin* open reading frame (885 bp), mouse *Scx* 3′ untranslated region (UTR; 291 bp), or mouse *type XII collagen* (500 bp) region was amplified by reverse transcription/polymerase chain reaction (RT-PCR) by using the following primers: *osteopontin*, 5′-ATGAGATTGGCAGTGATTTG-3′ and 5′-GTTGACCT CAGAAGATGAAC-3′; *Scx*, 5′-AAGAGGT GATGCCAC TAGTG-3′and 5′-TATACAAAATTTCCA GACTTTAT ATTATCAT-3′; *type XII collagen*, 5′-TCCCCATCAAA GAACAGACC-3′ and 5′-TGACTGCTGGATGA CAAAGG-3′. The amplicons for *osteopontin* and *Scx* were subsequently cloned into the pCRII vector (Invitrogen, Carlsbad, Calif., USA), and those for *type XII collagen* were cloned into pCR 4-TOPO (Invitrogen). A 623-bp mouse *periostin* cDNA fragment was isolated by RT-PCR with partial T7 and T3 promoter-containing primers (below, in italics) at the 5′ end and the 3′ end, respectively: T7: 5′-*CACTATAGGGC*GGCTGAA GATGGTTCCTCTC-3′, and T3: 5′-*CACTAAAGGGC* CATGTGGCTGTGTAAGG CATTC-3′. These cDNA fragments were further amplified by using the following adaptor primers to install full T7 and T3 promoter sequences into the fragments: 5′-GTAATAC GACTCAC TATAGGGC-3′ for T7, and 5′-AAT TAACCCTCAC TAAAGG-3′ for T3.

In situ hybridization

To generate antisense and sense digoxygenin-labeled riboprobes, linearized *osteopontin*, *Scx*, and *type XII collagen* plasmids and *periostin* cDNA fragments (see previous section) were transcribed by T7, T3, or Sp6 RNA polymerase as described elsewhere (Wilkinson 1995). Heads of P1 C57BL/6 mice were embedded in OCT compound (Sakura Finetechnical, Tokyo, Japan), and 10-μm-thick sagittal sections were cut. Mandibles of P35 mice were fixed in 4% paraformaldehyde at 4°C overnight, decalcified in 12.5% EDTA containing 2.5% paraformaldehyde for 6 weeks, and then embedded in OCT compound. In situ hybridization was carried out on these sections as previously described with some modification (Iseki et al. 1999). Polyvinyl alcohol was used as buffer during the color reaction.

RNA preparation and RT-PCR

Total RNA was isolated from cells by using ISOGEN (Nippon Gene, Tokyo, Japan) as described previously (Handa et al. 2002). cDNAs were synthesized from 1 μg total RNA in a 20-μl reaction volume containing 10× reaction buffer, 1 mM dNTP mixture, 1 U/μl RNase inhibitor, 0.25 U/μl reverse transcriptase (M-MLV reverse transcriptase; Invitrogen), and 0.125 μM random 9-mers (Takara, Tokyo, Japan). Amplification was performed in a PCR Thermal Cycler SP (Takara, Tokyo, Japan) for 25 cycles with the following reaction profile: 94°C for 1 min, 60°C for 30 s, and 72°C for 30 s. Synthesized cDNA served as a template for subsequent PCR amplification with mouse-specific primers: *bone sialoprotein* (*BSP*): sense 5′-AGGGAACTGACCAGTGTTGG-3′, antisense 5′-TCGTTGCCTGTTTGTTCGTA-3′; *osteocalcin* (*OC*): sense 5′-CATGAGGACCCTCTCTCTGC-3′, antisense 5′-GCCGGAGTCTGTTCACTACC-3′; *osteopontin*: sense 5′-TGCACCCAGATCCTATGACC-3′, antisense 5′-TGTGGTCATGGCTTTCATTG-3′; *periostin*: sense 5′-TTGAAGGTGTCCCGSCTTC-3′, antisense 5′-TGAT TCGTTCTTCCCGAGTC-3′; *Scx*: sense 5′-CTTTCTTC CACAAGCGGTCGT-3′, antisense 5′-TGTCACGGTCTT TGCTCAAC-3′; and *glyceraldehyde-3-phosphate dehydrogenase* (*GAPDH*): sense 5′-TGTTCCTACCCCCAA TTGTGT-3′, antisense 5′-AGGAGACAACCTGGTCC TCA-3′. Specific primers for *six-1*, *EphA4*, *GDF-5*, *collagen I* (*Coll*), and *osterix* have been described previously (Salingcamboriboon et al. 2003).

In vivo differentiation assay

The differentiation potential of $MDF^{E6\text{-}EGFP}$ cells was assessed by transplantation of the cells into SCID mice as described previously (Handa et al. 2002). Briefly, cells were inoculated subcutaneously into 5-week-old male CB-17 scid/scid (SCID) mice (Nihoncrea, Tokyo, Japan) after incubation of 1.5×10^6 cells in a mixture of 40 mg hydroxyapatite powder (Osferion, Olympus, Tokyo, Japan) and fibrin clot (mixture of mouse fibrinogen and thrombin: both from Sigma). Transplantation analysis was carried out three times, and three transplants were prepared per group. The mice were sacrificed after 4 weeks and subjected to

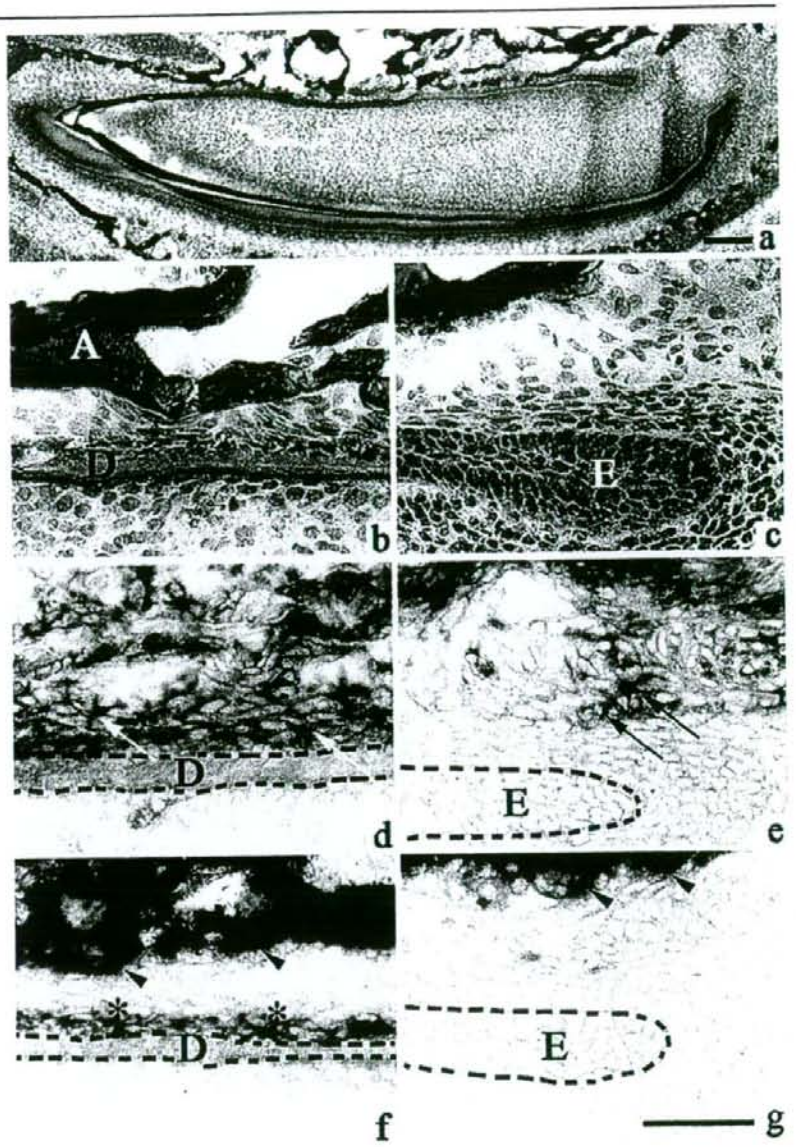

Fig. 1 In situ hybridization for *periostin* and *osteopontin* mRNA in newborn mice (*A* alveolar bone, *D* dentin, *E* dental epithelium). Sagittal sections of the incisor in the lower jaw of P1 mouse (**a**) were examined by hematoxylin and eosin staining (**a–c**) or in situ hybridization for *periostin* (**d, e**) or *osteopontin* (**f, g**). Higher magnifications of the anterior (**b, d, f**) and posterior (**c, e, g**) regions of the lingual side of the incisor are shown. Intense expression of *periostin* is seen in the developing PDL in the anterior region (**d**, *arrows*), with little expression in the posterior region (**e**, *arrows*). *Osteopontin* is expressed strongly throughout the alveolar bone (**f, g**, *arrowheads*) and in the differentiated cementoblasts in the anterior region (**f**, *asterisks*). No expression of *osteopontin* is observed in the dental follicle tissue in the posterior region (**g**). *Bars* 100 μm

histochemical analysis with immunohistochemical staining or in situ hybridization as described below. NIH3T3 cells were used for comparison.

Histochemical analysis

The transplants were fixed in 4% paraformaldehyde for 1 day, decalcified with 12.5% EDTA containing 2.5% paraformaldehyde for 3 days, and then embedded in OCT compound for the production of frozen sections. Subsequently, 30 serial sections of 5 μm in thickness were cut per implant and analyzed histochemically. Morphology was examined by hematoxylin and eosin staining. Observation by fluorescence microscopy (Axio imager, Carl Zeiss, Germany) was performed to distinguish between the cells of donor origin and host tissue. Expression of mRNA for *periosotin* and *Scx* was examined by in situ hybridization as described above. For immunohistocemical analysis, the

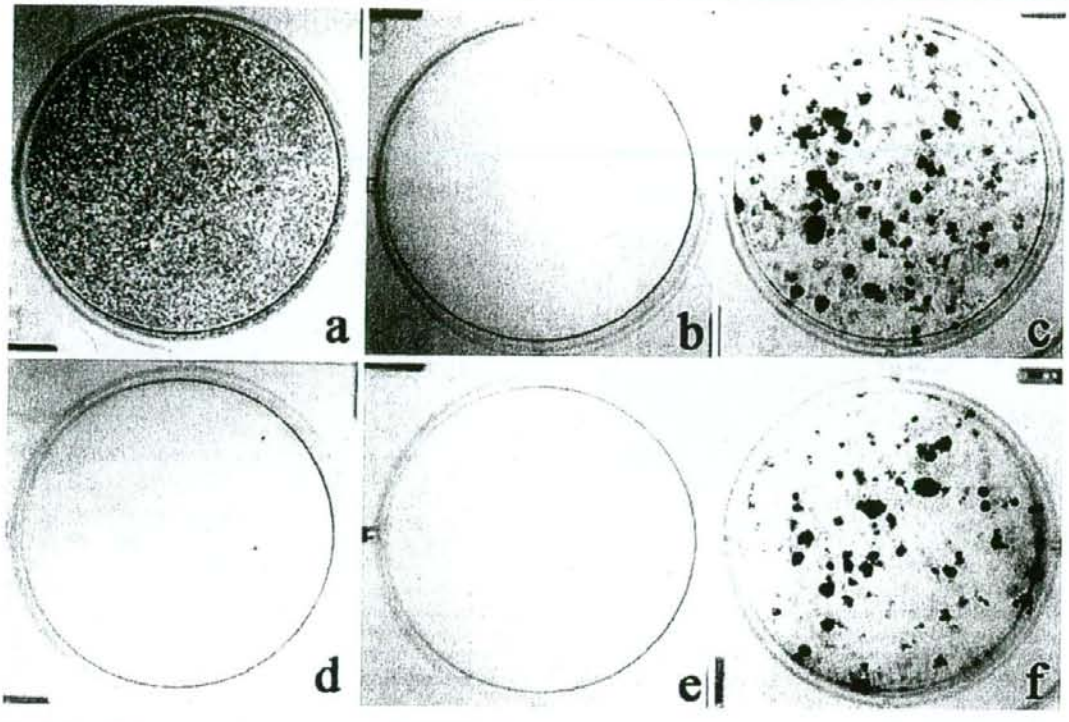

Fig. 2 ALP activity and mineralization potential of $MDF^{E6\text{-}EGFP}$ cells in vitro. $MDF^{E6\text{-}EGFP}$ cells were grown for 21 days in osteogenic differentiation medium in order to analyze ALP activity (**a–c**) and mineralization potential (**d–f**). High ALP activity by $MDF^{E6\text{-}EGFP}$ cells and MC3T3E1 (**a**, **c**) cells was apparent, whereas no activity was observed for NIH3T3 cells (**b**). Alizarin red staining showed no mineralized nodule formation for $MDF^{E6\text{-}EGFP}$ cells and NIH3T3 cells (**d**, **e**), whereas mineralized deposits were readily apparent for MC3T3E1 cells (**f**)

sections were blocked with 1% bovine serum albumin and probed with goat anti-type I collagen polyclonal antibody (Southern Biotech, Birmingham, Ala., USA) for 1 h. Sections were then probed with donkey anti-goat Alexa 555 (Invitrogen). After several washes, fluorescence in the sections was observed by fluorescence microscopy.

Results

Localization of periostin mRNA in the incisor tooth

Sequential developmental process of the dental follicle was observed in a sagittal section (in an anterior-posterior direction) of the P1 mice incisor (Fig. 1a). Immature cells were located posteriorly (Fig. 1c,e,g), and differentiation progressed toward the anterior region (Fig. 1b,d,f). To locate immature dental follicle cells, we first investigated the expression pattern of a PDL marker gene, *periostin*, and a cementoblast/osteoblast marker, *osteopontin*, in the lower incisor tooth germ of P1 mice. In a section stained with hematoxylin and eosin, dentin was seen in the anterior region (Fig. 1b), and invaginating dental epithelium was observed lingually in the posterior region (Fig. 1c). Intense expression of *periostin* was observed in the dental follicle cells close to the dentin layer in the anterior region (Fig. 1d, arrows). In contrast, only patchy expression of *periostin* was observed in the dental follicle cells in the posterior region (Fig. 1e, arrows). *Osteopontin* was expressed intensely throughout the alveolar bone (Fig. 1f,g, arrowheads). In accordance with the *periostin* expression pattern, *osteopontin* was expressed in the cementoblast adjacent to the dentin-forming layer in the anterior region (Fig. 1f, asterisks), but not in the posterior region (Fig. 1g). These data confirmed that the dental follicle cells in the posterior region were in an immature stage, whereas those in the anterior region were differentiated. We thus dissected dental follicle cells from the posterior region in order to establish a dental follicle progenitor cell culture system.

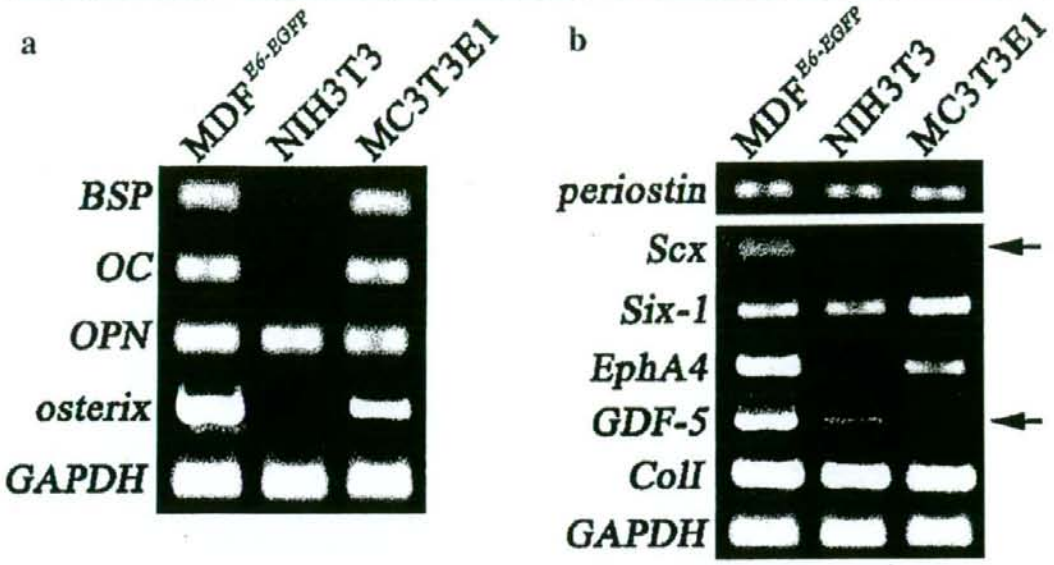

Fig. 3 RT-PCR analysis of $MDF^{E6\text{-}EGFP}$ cells. Expression of osteoblastic phenotype-related genes such as *bone sialoprotein* (*BSP*), *osteocalcin* (*OC*), *osteopontin* (*OPN*), and *osterix* (**a**), and PDL and tendon/ligament phenotype-related genes, such as *periostin*, *scleraxis* (*Scx*), *Six-1*, *EphA4*, *growth and differentiation factor 5* (*GDF5*), and *type I collagen* (*ColI*; **b**) were examined by RT-PCR analysis. Cells were cultured with osteoblastic differentiation (**a**) or normal medium (**b**), and total RNA was extracted (*arrows* strong expression of *Scx* and *GDF-5* in $MDF^{E6\text{-}EGFP}$ compared with NIH3T3 cells or MC3T3E1 cells)

Characterization of $MDF^{E6\text{-}EGFP}$ cells

MDF cells were isolated from the posterior region of the incisor tooth germ, and their life span was extended by using a retrovirus-expressing human papillomavirus type 16 (HPV16) *E6* gene lacking the PDZ-domain-binding motif ($E6^{\Delta 146\text{-}151}$), together with a lentivirus expressing *EGFP* for fluorescence detection. After viral infection, the expression of $E6^{\Delta 146\text{-}151}$ was confirmed by RT-PCR analysis (data not shown). $MDF^{E6\text{-}EGFP}$ cells maintained their original morphology and cell proliferation activity, even when the cells were cultured beyond population doubling (PD) 150, indicating that they had overcome replicative senescence. In contrast, normal MDF cells were only able to propagate until PD 10 (data not shown). We thus used $MDF^{E6\text{-}EGFP}$ cells for further analysis.

To assess the osteogenic potential of $MDF^{E6\text{-}EGFP}$ cells, the cells were treated with osteogenic differentiation medium supplemented with ascorbic acid, β-glycerophosphate, and dexamethasone for 21 days. ALP activity was observed in $MDF^{E6\text{-}EGFP}$ cells (Fig. 2a) and in osteoblast-like MC3T3E1 cells (Fig. 2c). Mineralized nodule formation by the $MDF^{E6\text{-}EGFP}$ cells was not observed (Fig. 2d), whereas MC3T3E1 cells were able to deposit mineralized nodules (Fig. 2f). Neither ALP activity nor mineral deposition was observed in the fibroblastic cells (NIH3T3 cells; Fig. 2b,e). RT-PCR analysis was performed to characterize the $MDF^{E6\text{-}EGFP}$ cells by using primers for osteoblast phenotype-related genes *BSP*, *OC*, and *osterix*. $MDF^{E6\text{-}EGFP}$ cells expressed all of these osteoblast marker genes, with a similar expression pattern to that of MC3T3E1 cells. In contrast, no expression of osteoblast phenotype-related genes was observed in NIH3T3 cells, except for *BSP*. From these data, we considered that osteoblastic populations were present in $MDF^{E6\text{-}EGFP}$ cells (Fig. 3a).

To characterize the PDL-forming properties of $MDF^{E6\text{-}EGFP}$ cells, gene expression of *periostin* and tendon/ligament phenotype-related genes encoding *Scx*, *EphA4*, *Six-1*, *GDF-5*, and *ColI* were examined by RT-PCR analysis. $MDF^{E6\text{-}EGFP}$ cells expressed all of these genes suggesting that they possessed PDL and tendon cell properties (Fig. 3b). Stronger expression of *Scx* and *GDF-5* was observed in $MDF^{E6\text{-}EGFP}$ cells than in NIH3T3 cells or MC3T3E1 cells (Fig. 3b, arrows). Expression patterns of *Scx* and *periostin* mRNA were examined in postnatal (P35) mouse molar PDL (Fig. 4a) by in situ hybridization. Intense expression of *periostin* was observed throughout the PDL (Fig. 4b, arrows), and *Scx* was also expressed in the PDL (Fig. 4c, arrowheads).

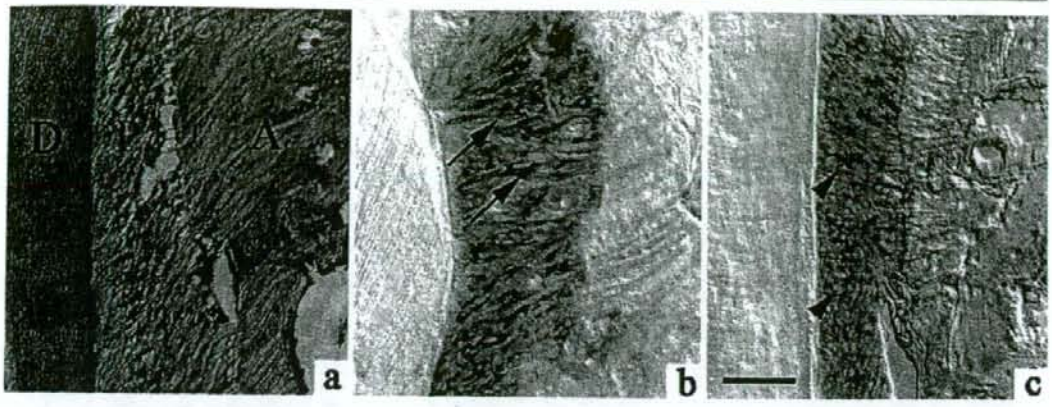

Fig. 4 In situ hybridization for *Scx* and *periostin* mRNA in postnatal PDL (*A* alveolar bone, *D* dentin, *P* PDL). Frontal sections of the molar tooth of P35 mouse (**a**) were examined by hematoxylin and eosin staining (**a**) or in situ hybridization with *periostin* (**b**) or *Scx* (**c**). Intense expression of *periostin* was seen within PDL (**b**, *arrows*). Expression of *Scx* can be seen throughout the PDL (**c**, *arrowheads*). *Bars* 100 μm

In vivo characterization of MDF$^{E6\text{-}EGFP}$ cells

To investigate the differentiation potential of MDF$^{E6\text{-}EGFP}$ cells, the cells were implanted into SCID mice. After 4 weeks, MDFE6-EGFP cell transplants formed PDL-like fibrous tissue (Fig. 5a-a) including scattered bone-like tissue formation (Fig. 5a-b). The PDL-like tissues resembled the structure of PDL with sheet-like cells (Fig. 5a-a, a-d, arrows). Cells within the PDL- and bone-like tissues were strongly positive for EGFP (Fig. 5a-d, a-e). In contrast, no such tissues were formed in the transplants without mouse cells (HAP transplants; Fig. 5a-f). Immunohistochemical staining revealed dense type I collagen fibril assembly in the PDL-like tissue (Fig. 5b-a), whereas type I collagen fibril assembly was not evident in the NIH3T3 cell or HAP transplants (Fig. 5b-b, b-c). To validate the capacity of MDF$^{E6\text{-}EGFP}$ cells to differentiate into PDL in vivo, the expression of *periostin* and *Scx* was examined in the transplants by in situ hybridization. Expression of *type XII collagen* has been shown in the PDL during tooth root formation; therefore, we also examined the expression of this gene in the transplants (MacNeil et al. 1998). As expected, the expression of *periostin*, *Scx*, and *type XII collagen* was observed in MDF$^{E6\text{-}EGFP}$ cells (Fig. 6a,d,g, arrows), whereas these genes were not expressed in the NIH3T3 cell transplants (Fig. 6b,e,h) or HAP transplants (Fig. 6c,f,i). All the transplants except HAP transplants were EGFP-positive, indicating that cells within the MDF$^{E6\text{-}EGFP}$ and NIH3T3 transplants had originated from the donor (Fig. 6j,k,l).

Discussion

We have immortalized dental follicle cells from cells isolated from mice incisor tooth germs. These cells express *Scx*, *GDF-5*, *EphA4*, *Six-1*, and *Coll*, which are expressed in a developing tendon (Bonnin et al. 2005; Brent et al. 2003; Luukko et al. 2005; Settle et al. 2003). Our findings also suggest that MDF$^{E6\text{-}EGFP}$ cells act as PDL progenitors since they form a PDL-like structure that expresses *periostin*, *Scx*, and *type XII collagen* and that is capable of producing dense collagen fibril assembly in vivo.

In the present study, MDF$^{E6\text{-}EGFP}$ cells have been isolated from the undifferentiated dental follicle region of the incisor in which there is minimal expression of *periostin* and no expression of *osteopontin*. Our findings indicate that MDF$^{E6\text{-}EGFP}$ cells act as PDL progenitors, as shown by their capacity to generate PDL-like tissue in vivo. MDF$^{E6\text{-}EGFP}$ cells are similar to tendon progenitors with respect to their expression of *Scx* and *GDF-5*, a marker for tendon/ligament. Since PDL is morphologically similar to the tendon/ligament in vivo, dental follicle cells may have a similar phenotype as tendon progenitors. The expression of *Scx* by mouse PDL has been seen in the present study, suggesting that the PDL has some characteristics similar to tendon. Salingcamboriboon and coworkers (2003) have reported that a tendon-derived cell line isolated from mouse Achilles tissue shows expression of *Scx*, and that these cells are able to form tendon-like tissue when they are implanted into a mouse tendon-defect model. MDF$^{E6\text{-}EGFP}$ cells show a similar phenotype to these cells, and the transplants form PDL-like tissues comprising cells

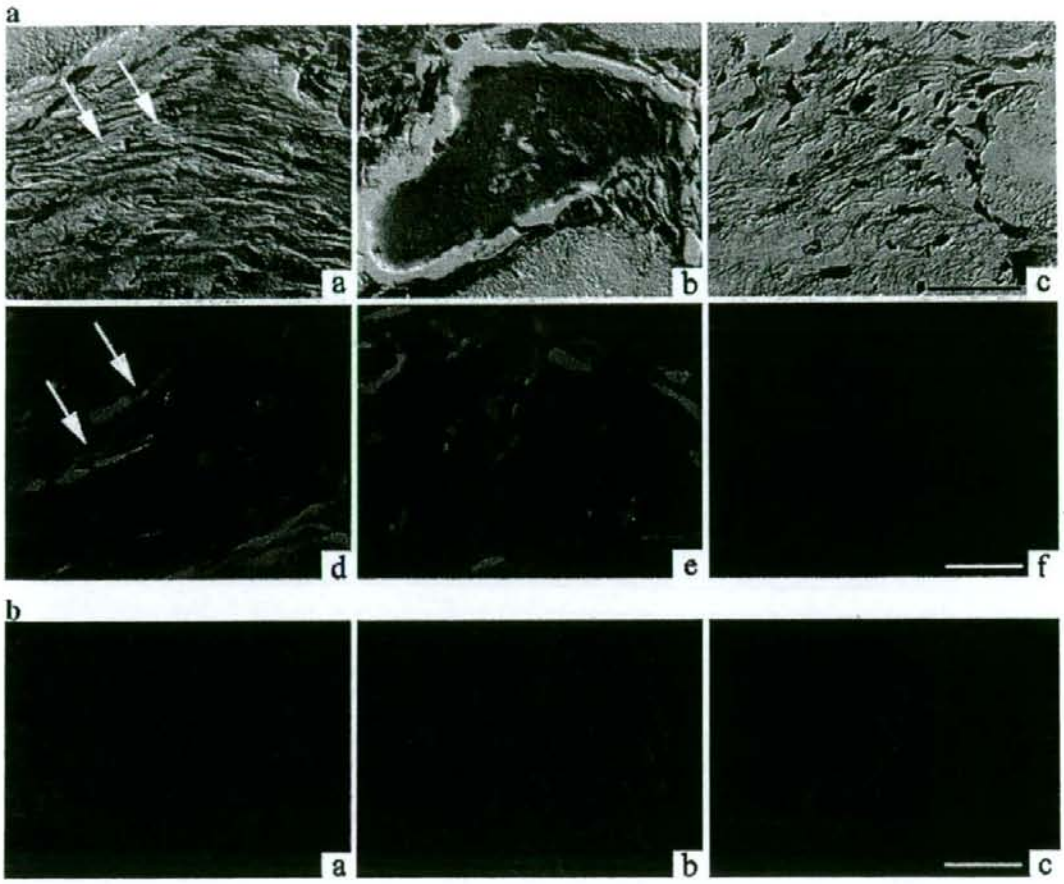

Fig. 5 Differentiation potential of MDF$^{E6\text{-}EGFP}$ cells in vivo. **a** Representative sections of MDF$^{E6\text{-}EGFP}$ cell transplants (**a-a**, **a-b**, **a-d**, and **a-e**) and transplants without mouse cells (HAP transplants; **a-c**, **a-f**). The transplant was stained with hematoxylin and eosin (**a–a** to **a-c**) or viewed for EGFP fluorescence (**a-d** to **a-f**). PDL-like fibrous tissues (**a-a**, **a-d**, *arrows*) and bone-like tissues (**a-e**) are visible in the MDF$^{E6\text{-}EGFP}$ transplants. Cells within the MDF$^{E6\text{-}EGFP}$ transplants are positive for EGFP (**a-d**, **a-e**). **b** Immunohistochemical staining with anti-type I collagen polyclonal antibody in the MDF$^{E6\text{-}EGFP}$ transplants (**b-a**), NIH3T3 cell transplants (**b-b**), or HAP transplants (**b-c**) are shown. Dense type I collagen fibril assemblies are seen in the MDF$^{E6\text{-}EGFP}$ transplants. *Bars* 50 μm

with sheet-like extensions surrounding a densely packed, collagen fibril assembly. Our data are also coincident with previous findings that human PDL cells are able to form PDL-like tissue upon implantation into immunodeficient mice for 4 weeks, suggesting that the differentiation potential of MDF$^{E6\text{-}EGFP}$ is comparable with these cells (Grzesik et al. 2000; Seo et al. 2004). In the present study, the PDL differentiation of MDF$^{E6\text{-}EGFP}$ cells has been assessed by the expression of *periostin*, *Scx*, and *type XII collagen* (Bohme et al. 1995; Karimbux and Nishimura 1995). The expression of *periostin* is observed in both alveolar bone cells and dental follicle cells on P1. However, previous findings and our data have shown that the expression of *periostin* is limited to the adult periodontal ligament, indicating that it could be used as a marker for differentiated PDL (Kruzynska-Frejtag et al. 2004). In the case of MDF$^{E6\text{-}EGFP}$ transplants, they form PDL-like tissue expressing *periostin*, *Scx*, and *type XII collagen*, thus indicating that the tissue is almost identical to PDL. From these findings, we suggest that the MDF$^{E6\text{-}EGFP}$ cells have PDL progenitors able to differentiate into PDL in vivo. Although the role of the tendon/ligament related genes in PDL development is not clear, these data strongly support our hypothesis that MDF$^{E6\text{-}EGFP}$ cells possess PDL progenitors that resemble tendon progenitors.

Progenitors for cementoblasts, PDL cells, and osteoblasts are generally believed to be present in dental follicle cells (Ten Cate 1994), and we have previously shown that

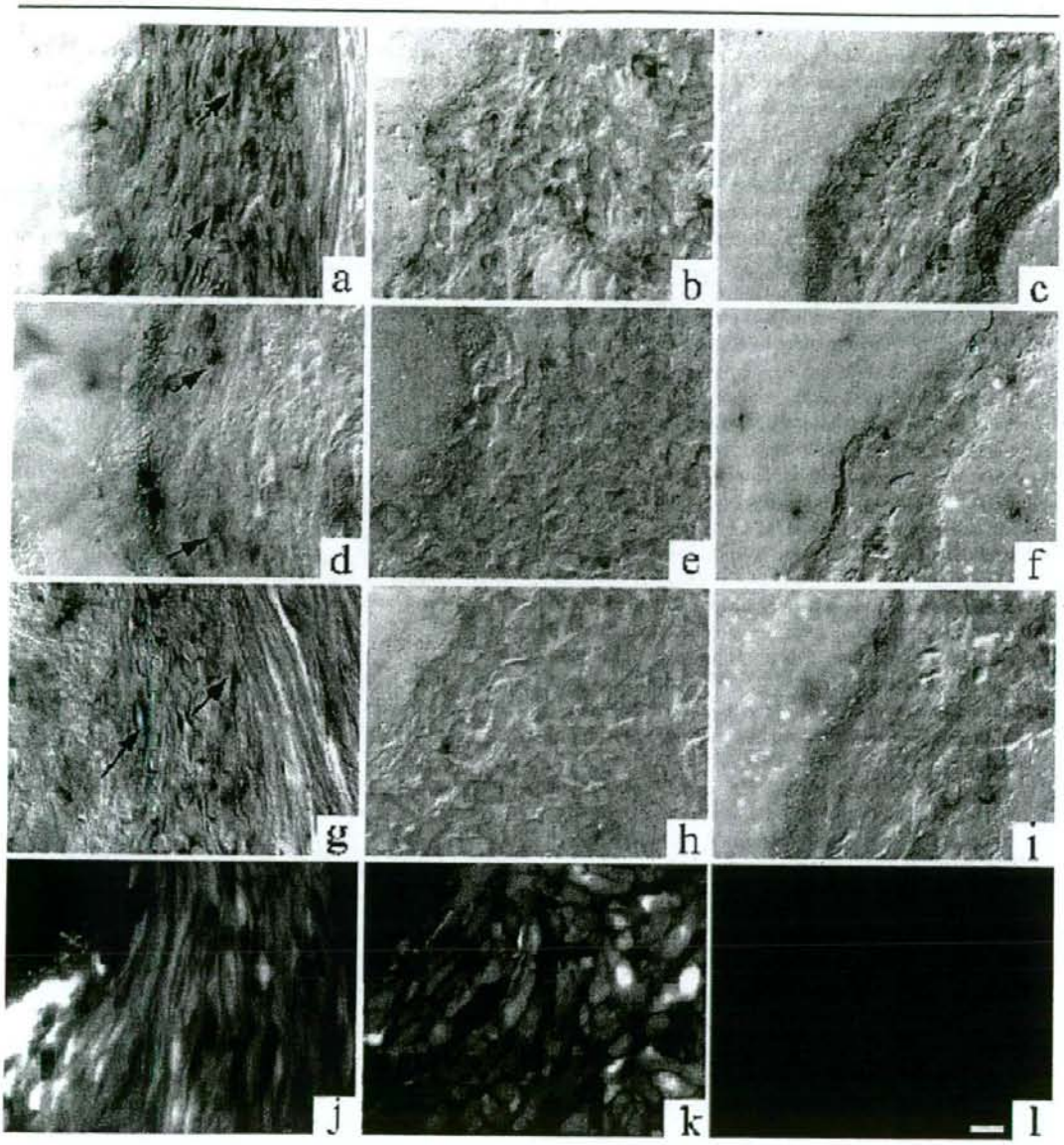

Fig. 6 In situ hybridization for *periostin*, *Scx*, and *type XII collagen* mRNA in MDF$^{E6\text{-}EGFP}$ cell transplants. Representative sections of MDF$^{E6\text{-}EGFP}$ cell transplants (**a**, **d**, **g**, **j**), NIH3T3 cell transplants (**b**, **e**, **h**, **k**), and transplants without mouse cells (HAP transplants; **c**, **f**, **i**, **l**) were analyzed by in situ hybridization for *periostin* (**a**–**c**), *Scx* (**d**–**f**), or *type XII collagen* (**g**–**i**), or viewed for EGFP fluorescence (**j**–**l**). Expression of *periostin*, *Scx*, or *type XII collagen* is seen in the MDF$^{E6\text{-}EGFP}$ transplants (**a**, **d**, **g**, *arrows*). Cells within the MDF$^{E6\text{-}EGFP}$ and NIH3T3 transplants are positive for EGFP (**j**, **k**). *Bar* 100 μm

cementoblast progenitors can be obtained from bovine dental follicle tissues (Handa et al. 2002). Cementoblast differentiation does not occur in MDF$^{E6\text{-}EGFP}$ cell transplants. This discrepancy may be explained by the isolation technique used for MDF$^{E6\text{-}EGFP}$ cells. The cells grown from mouse dental follicle tissues have been employed in this study, whereas in a previous study, we isolated bovine dental follicle cells by bacterial collagenase digestion; this

suggests that isolation of cementoblast progenitors requires enzyme digestion (Handa et al. 2002). We have also found that $MDF^{E6\text{-}EGFP}$ cells can act as osteoblast progenitors, since they form bone-like tissue in vivo. Although $MDF^{E6\text{-}EGFP}$ cells express an array of osteoblast marker genes, they cannot form mineralized nodules in vitro, as described previously for bovine dental follicle cells (Handa et al. 2002). This may be because the difference in time required for the calcification of MDF^{E6EFGP}. The timing and extent of mineralization varies substantially depending on the origin of the cells or experimental conditions. Mineralization of MDF^{E6EFGP} may require a longer period compared with that for MC3T3E1. Recently, Yoshizawa et al. (2004) have reported that PDL cells do not have the ability to form mineralized nodules, and Msx-2 plays a central role in suppressing matrix mineralization in these cells. Our findings suggest that PDL progenitors present in $MDF^{E6\text{-}EGFP}$ cells are similar to those in PDL, and that the cells preventing or delaying the mineralization of osteoblast progenitors are also present in $MDF^{E6\text{-}EGFP}$ cells. Based on these findings, future studies are necessary to elucidate the mechanism by which $MDF^{E6\text{-}EGFP}$ cells differentiate into osteoblastic cells. From our present findings, we suggest that PDL progenitors and osteoblast progenitors co-exist in $MDF^{E6\text{-}EGFP}$ cells. In addition, the slight expression of BSP observed in NIH3T3 cells might be attributable to the effect of the osteogenic differentiated medium.

Normal MDF cells proliferate in culture for a finite number of PD because of cellular senescence. Therefore, attempts have been made to establish immortalized MDF cells in order to analyze their differentiation potential. A deficiency in p53 is sufficient for the establishment of mouse clonal cell lines from various tissues (Hanazono et al. 1997). HPV16E6 has been shown to abrogate the function of p53 and has the ability to immortalize various cell types (Fehrmann and Laimins 2003; Kiyono et al. 1998). However, it also has other biological functions that depend on its C-terminal PDZ-domain-binding motif, such as cell transformation and skin hyperplasia in transgenic mice (Nguyen et al. 2003). For instance, mice expressing HPV-16 E6 in their epidermis develop epithelial hyperplasia and squamous carcinomas (Song et al. 1999). However, transgenic mice expressing HPV-16 E6 lacking the PDZ-binding motif fail to display epithelial hyperplasia but retain the ability to inactivate p53 (Nguyen et al. 2003). In the present study, we have used a mutant version of E6 that lacks the C-terminal PDZ-domain binding-motif to extend the life span of MDF cells and have succeeded in immortalizing MDF cells without affecting their differentiation potential. In addition, we have confirmed that no tumor formation occurs in $MDF^{E6\text{-}EGFP}$ cell transplants (data not shown). This suggests that the immortalization system used in this study might be useful for the immortalization of MDF cells.

In summary, we have established an immortalized mouse dental follicle cell culture system that possesses PDL progenitors. $MDF^{E6\text{-}EGFP}$ cells might provide new insights into the mechanisms of PDL formation, including those pertaining to PDL cell differentiation. They may also be a powerful tool in the development of therapeutic strategies for the treatment of periodontitis.

Acknowledgement We are grateful to Dr. Masato Yamauchi for his advice and discussions during the course of this work.

References

Bohme K, Li Y, Oh PS, Olsen BR (1995) Primary structure of the long and short splice variants of mouse collagen XII and their tissue-specific expression during embryonic development. Dev Dyn 204:432–445

Bonnin MA, Laclef C, Blaise R, Eloy-Trinquet S, Relaix F, Maire P, Duprez D (2005) Six1 is not involved in limb tendon development, but is expressed in limb connective tissue under Shh regulation. Mech Dev 122:573–585

Bosshardt DD, Schroeder HE (1996) Cementogenesis reviewed: a comparison between human premolars and rodent molars. Anat Rec 245:267–292

Brent AE, Schweitzer R, Tabin CJ (2003) A somitic compartment of tendon progenitors. Cell 113:235–248

Chai Y, Jiang X, Ito Y, Bringas P Jr, Han J, Rowitch DH, Soriano P, McMahon AP, Sucov HM (2000) Fate of the mammalian cranial neural crest during tooth and mandibular morphogenesis. Development 127:1671–1679

D'Errico JA, Ouyang H, Berry JE, MacNeil RL, Strayhorn C, Imperiale MJ, Harris NL, Goldberg H, Somerman MJ (1999) Immortalized cementoblasts and periodontal ligament cells in culture. Bone 25:39–47

Fehrmann F, Laimins LA (2003) Human papillomaviruses: targeting differentiating epithelial cells for malignant transformation. Oncogene 22:5201–5207

Grzesik WJ, Cheng H, Oh JS, Kuznetsov SA, Mankani MH, Uzawa K, Robey PG, Yamauchi M (2000) Cementum-forming cells are phenotypically distinct from bone-forming cells. J Bone Miner Res 15:52–59

Hanazono M, Tomisawa H, Tomooka Y, Hirabayashi K, Aizawa S (1997) Establishment of uterine cell lines from p53-deficient mice. In Vitro Cell Dev Biol Anim 33:668–671

Handa K, Saito M, Yamauchi M, Kiyono T, Sato S, Teranaka T, Sampath Narayanan A (2002) Cementum matrix formation in vivo by cultured dental follicle cells. Bone 31:606–611

Horiuchi K, Amizuka N, Takeshita S, Takamatsu H, Katsuura M, Ozawa H, Toyama Y, Bonewald LF, Kudo A (1999) Identification and characterization of a novel protein, periostin, with restricted expression to periosteum and periodontal ligament and increased expression by transforming growth factor beta. J Bone Miner Res 14:1239–1249

Iseki S, Wilkie AO, Morriss-Kay GM (1999) Fgfr1 and Fgfr2 have distinct differentiation- and proliferation-related roles in the developing mouse skull vault. Development 126:5611–5620

Karimbux NY, Nishimura I (1995) Temporal and spatial expressions of type XII collagen in the remodeling periodontal ligament during experimental tooth movement. J Dent Res 74:313–318